「ヒト肺腺癌細胞の放射線応答制御におけるミトコンドリア関連因子の役割に関する研究」

弘前大学大学院保健学研究科保健学専攻

提出者氏名：　佐 藤 嘉 晃

所　　属：　放射線技術科学領域

指導教員：　敦 賀 英 知

目次

Abbreviations

ATP: Adenosine triphosphate

ATM: Ataxia-telangiectasia mutated

ATR: ATM and RAD3-related

Chk1: Checkpoint kinase 1

DAP3: Death-associated protein 3

DMSO: Dimethyl sulfoxide

Drp1: Dynamin-related protein 1

ECL: Enhanced chemiluminescent

EIF-2α: Eukaryotic initiation factor-2α

FBS: Fetal bovine serum

FITC: Fluorescein isothiocyanate

HRP: Horseradish peroxidase

IFN: Interferon

IR: Ionizing radiation

L-OPA1: Long isoform OPA1

LUAD: Lung adenocarcinoma

Mfn (1/2): Mitofusin-1/2

MtDNA: mitochondrial DNA

OPA1: Optic atrophy protein 1

PBS(–): Ca^{2+} and Mg^{2+} free phosphate-buffered saline

Pchk1: Phosphorylated chk1

PeIF-2α: Phosphorylated eIF-2α

PH3: Phosphorylated-histone H3

PI: Propidium iodide

Poly(I:C)-HMW: Polyinosinic-polycytidylic acid-high molecular weight/LyoVec™

QRT-PCR: Quantitative reverse transcription polymerase chain reaction

RIG-I: Retinoic acid-inducible gene-I

RLR: RIG-I-like receptor

SD: standard deviation

TCGA: The cancer genome atlas

序論

ミトコンドリアはエネルギー産生を担う重要な細胞小器官である. ミトコンドリアは, 独自の DNA 及びリボソームを有しており, また融合と分裂を繰り返している. これらのミトコンドリアの特徴は, エネルギー産生に加え, 細胞死や免疫応答などの細胞機能においも深く関わっている. 例えば, C 型肝炎ウイルスはミトコンドリアを融合させることで, 感染細胞のアポトーシスを回避することが報告されている. また, ミトコンドリアの分裂は乳がん細胞の放射線感受性制御に関与することが報告されている. このように, ウイルス感染や放射線などのストレス応答におけるミトコンドリアの重要性が明らかになっている.

Retinoic acid-inducible gene-I (RIG-I) 様受容体 (RIG-I-like receptor: RLR) は細胞質のウイルスセンサーとして機能し, ウイルスに対する生体防御機構において重要な役割を果たす. RLR には RIG-I および melanoma differentiation associated gene 5 などがあり, これら受容体が二本鎖 RNA や 5`-三リン酸 RNA などのウイルス由来核酸を認識すると, ミトコンドリア外膜上に発現するアダプター分子 mitochondrial antiviral signaling protein に情報が伝達される. その後, 下流のシグナル伝達が活性化されることで, I 型インターフェロンや炎症性サイトカインの産生を介して抗ウイルス応答が誘導される.

近年では RLR が抗ウイルス応答だけではなく, 肺癌を含む様々な癌細胞に対して抗腫瘍免疫活性および細胞死を誘導することが明らかになり, RLR に着目した癌治療戦略が期待されている. これまで所属研究室では, RLR 刺激因子がヒト非肺腺癌細胞の放射線感受性を増強させること, RLR 刺激因子と X 線の併用処理が相乗的に細胞死を誘導することを報告した. このことから, RLR 刺激因子は細胞の放射線応答を制御することが示唆されたが, ヒト肺腺癌細胞においてミトコンドリアが RLR 刺激因子による放射線応答制御機構にどのような関与しているのかは未解明である.

本研究では, ミトコンドリア関連因子に着目して, ヒト肺腺癌細胞における RLR 刺激因子による放射線応答制御機構の詳細な分子機構の解明を目指した. さらに, その研究成果からミトコンドリアリボソームタンパク質 death-associated protein 3 (DAP3) がヒト肺腺癌細胞の新たな放射線抵抗性因子であることが見出されたため, 主要な放射線抵抗性因子である細胞周期制御や DNA 損傷応答に着目して DAP3 を介した放射線応答制御機構の解明を目指した. 本論文は以下に述べる第一章から第二章で構成される.

≪第一章≫「ヒト肺腺癌細胞における RIG-I 様受容体刺激因子による DAP3 を介した放射線応答制御に関する研究」

はじめにミトコンドリア融合および分裂因子と DAP3 のタンパク質発現を解析したところ, RLR 刺激因子で処理したヒト肺腺癌細胞 A549 ではこれらタンパク質の発現が減少していることを見出した. そこで, RNA 干渉法により調製した各タンパク質発現抑制細胞を用いて実験を行ったところ,

(i) DAP3 がヒト肺腺癌細胞（A549 と H1299）の放射線抵抗性に関与していること, (ii) DAP3 の発現抑制細胞では放射線による細胞死が増加し, その結果 RLR 刺激因子による放射線誘発細胞死増強効果が減弱することが明らかとなった. さらに, mRNA 及びタンパク発現解析から, RLR 刺激因子は mRNA の翻訳抑制に関わる eukaryotic initiation factor-2α のリン酸化を促進させることで DAP3 のタンパク質発現を抑制することが示唆された.

以上の結果より, RLR 刺激因子は DAP3 のタンパク質発現を減少させることでヒト肺腺癌細胞の放射線応答を制御することが示唆された.

≪第二章≫「DAP3 を介した放射線照射後の細胞周期制御とヒト肺腺癌細胞の放射線抵抗性との関連」

DAP3は放射線高感受性を示すataxia-telangiectasia-mutated欠損細胞に放射線抵抗性を付与する因子としてクローニングされたが, DAP3を介した放射線抵抗性制御機構は未解明である. 放射線抵抗性に関わる細胞周期およびDNA損傷応答制御とDAP3との関連について解析した結果, (i) DAP3の発現を抑制したヒト肺腺癌細胞では照射後のG2/M期停止が抑制されること, (ii) DAP3の発現抑制によりG2/M期の制御因子cdc2のリン酸化とその上流の制御因子checkpoint kinase 1 (chk1) の照射後のリン酸化の亢進が減少することが明らかになった. そこで照射後のG2/M期停止に着目して解析を進めた結果, (i) 照射後のG2/M期停止にはchk1が重要であること, (ii) chk1阻害剤で処理したH1299は放射線高感受性を示すこと, A549に関しては, chk1阻害剤によるG2/M期停止の解除に加え, chk2阻害剤により放射線抵抗性因子p21の照射後の発現増加を抑制した場合に放射線感受性が高まることが明らかになった.

以上の結果より, DAP3はchk1を介して放射線誘発G2/M期停止を誘導することでH1299の放射線抵抗性を制御していることが示唆された. 一方, A549に対してはDAP3がchk1とchk2を介したイベントを通して放射線抵抗性を制御している可能性が示唆された.

Chapter 1. DAP3 is involved in modulation of cellular radiation response by RIG-I-like receptor agonist in human lung adenocarcinoma cells

Introduction

Mitochondria are essential organelles for regulating cellular functions, such as oxidative phosphorylation, cell death, and immune responses[1,2]. Mitochondria are highly dynamic organelles that undergo fusion and fission, referred to as mitochondrial dynamics[3]. These processes are regulated by several proteins[3], e.g., mitochondrial fusion is mainly regulated by mitofusin-1/2 (Mfn1/2) and optic atrophy protein 1 (OPA1), with the former involved in outer membrane fusion and the latter in inner membrane fusion, whereas dynamin-related protein 1 (Drp1) is the main protein that initiates mitochondrial fission. In addition, the mitochondria contain their own DNA and ribosomes that synthesize mitochondrial DNA (mtDNA)-encoded proteins[4]. These characteristics have been reported to be important in self-maintenance of mitochondrial functions in response to various stress conditions such as viral infection[5-7].

Retinoic acid-inducible gene-I (RIG-I)-like receptors (RLRs) are pattern-recognition receptors that recognize pathogen-associated molecular patterns in the cytosolic fraction. RLRs detect viral RNA and elicit anti-viral responses, such as the induction of type I interferons (IFNs) through the adaptor molecule mitochondrial anti-viral signaling protein located in the mitochondrial membrane[8,9]. Furthermore, recent studies have shown that RLR activation induces anti-tumor effects, including anti-tumor immunity and cell death in various cancer types, such as lung cancer[10-12]. Therefore, strategies for cancer therapy focusing on RLR activation have been studied[12-14].

Our previous report showed that the RLR agonist synthetic double-stranded RNA Poly(I:C)-HMW/LyoVec™ (Poly(I:C)) enhanced radiosensitivity and that cotreatment with Poly(I:C) and ionizing radiation (IR) exerted a more-than-additive effect for each treatment alone in inducing cell death in human lung adenocarcinoma cells[15]. These results indicate that Poly(I:C) modulates cellular radiation responses. However, it remains unknown how mitochondria are involved in the modulation of cellular radiation responses by Poly(I:C) in human lung adenocarcinoma cells.

Growing evidence has demonstrated that mitochondrial dynamics and mitochondrial ribosome proteins are involved in cellular responses to various stresses, including radiation and viral infection[5, 16-19]. For example, it has been reported that mitochondrial fission-related proteins are involved in the radiosensitivity of EMT6 murine breast cancer cells[16]. In addition, mitochondrial dynamics are reported to regulate RLRs-mediated antiviral immune response[5]. Moreover, Kim et al. reported that Hepatitis C virus causes mitochondrial fission, which leads to evasion of apoptosis in huh-7 human hepatocellular carcinoma cells[17]. Among mitochondrial ribosome proteins, death-associated protein 3 (DAP3; mitochondrial ribosome protein S29) is known as a GTP-binding protein

and a major positive mediator of cell death[18]. Conversely, Henning reported that overexpression of DAP3 conferred radioresistance to ataxia telangiectasia cells exhibiting high radiosensitivity[19]. Considering these findings, we hypothesized that the RLR agonist Poly(I:C) modulates the cellular radiation response by regulating mitochondrial dynamics or the mitochondrial ribosome protein DAP3. To address this hypothesis, we investigated the relationship between mitochondrial dynamics, DAP3, and the modulation of the cellular radiation response by Poly(I:C) in human lung adenocarcinoma cells.

The major findings of this study were as follows: (i) Poly(I:C) decreased the expression of mitochondrial dynamics-related proteins and DAP3 in human lung adenocarcinoma cells; (ii) DAP3 was involved in the resistance of lung adenocarcinoma cells to IR-induced cell death, whereas mitochondrial dynamics were not; (iii) a more-than-additive effect of cotreatment with Poly(I:C) and IR on increasing cell death was diluted by DAP3-knockdown because of an increase in cell death induced by IR alone. These findings suggest that the RLR agonist Poly(I:C) modulates cellular radiation response of lung adenocarcinoma cells by downregulating DAP3 protein expression.

Materials & Methods

1. Reagents

Calcium^{2+} and magnesium2^{+} free phosphate-buffered saline was purchased from Wako Pure Chemical Industries, Ltd. (Osaka, Japan). Propidium iodide (PI) was purchased from Sigma-Aldrich (Merck KGaA, Darmstadt, Germany). Poly(I:C)-HMW/LyoVec™ (Poly(I:C)), which is a complex of the synthetic double-stranded RNA analog poly(I:C) and a transfection reagent (LyoVec™), were purchased from InvivoGen (San Diego, CA, USA). Annexin V-FITC was purchased from BioLegend, Inc. (San Diego, CA, USA). The anti-rabbit horseradish peroxidase (HRP)-conjugated IgG (cat. no. 7074), and the anti-mouse HRP-conjugated IgG (cat. no. 7076) secondary antibodies, anti-Mfn1 (cat. no. 14739), anti-OPA1 (cat. no. 80471), anti-Drp1 (cat. no. 5391), anti-eIF-2α (cat. no. 9722), anti-phospho-eIF-2α (cat. no. 3597), anti-β-actin (cat. no. 4967) monoclonal antibodies, and SignalSilence® Mfn1 (cat. no. 13303) siRNA were purchased from Cell Signaling Technology Inc. (Danvers, MA, USA). Anti-DAP3 (cat. no. 610662) monoclonal primary antibody was purchased from BD Biosciences (Franklin Lakes, NJ, USA). Ambion Silencer® Select Pre-designed siRNA against the gene-encoding Drp1 (cat. no. s19560), the gene-encoding DAP3 (cat. no. s1506), and Silencer® Select Negative #1 Control (cat. no. AM4611) siRNAs were purchased from Thermo Fisher Scientific, Inc. (Waltham, MA, USA).

2. Cell culture and treatment

Human lung adenocarcinoma cells A549 and H1299 were purchased from Riken Bio-Resource Center (Tsukuba, Japan) and American Type Culture Collection (Manassas, VA, USA), respectively. A549 cells were maintained in Dulbecco's modified Eagle's medium (Sigma-Aldrich) supplemented with 1% penicillin/streptomycin (Wako Pure Chemical Industries, Ltd.) and 10% heat-inactivated fetal bovine serum (Sigma-Aldrich) at 37 °C in a humidified atmosphere of 5% CO_2. H1299 cells were maintained in RPMI1640 medium (Gibco®; Invitrogen/Thermo Fisher Scientific, Waltham, MA, USA) supplemented with 1% penicillin/streptomycin and 10% heat-inactivated FBS at 37 °C in a humidified atmosphere of 5% CO_2.

Cells were seeded onto 35-mm culture dishes (6.0×10^4 cells) or 60-mm culture dishes (1.2×10^5 cells) (Sumitomo Bakelite Co., Ltd., Tokyo, Japan) and were cultured for 6 h to allow adherence. After incubation, the RLR agonist Poly(I:C) (250 ng/mL) was added to the culture medium for the indicated time periods. Next, the cells were harvested using 0.1% trypsin-ethylenediaminetetraacetic acid (Wako Pure Chemical Industries, Ltd.) for subsequent analysis. In some experiments, X-ray irradiation was performed 1 h after Poly(I:C) administration, and the treated cells were cultured.

3. In vitro X-ray irradiation

Cells were irradiated (150 kVp; 20 mA; 0.5-mm Al filter and 0.3-mm Cu filter) using an X-ray generator (MBR-1520R-3; Hitachi, Ltd., Tokyo, Japan) at a distance of 45 cm from the focus and a dose rate of 0.99–1.02 Gy/min.

4. SDS-PAGE and western blotting

SDS-PAGE and western blot analysis were performed as previously reported[20]. The following primary antibodies were used: anti-Mfn1 (1:3,000), anti-OPA1 (1:3,000), anti-Drp1 (1:3,000), anti-DAP3 (1:3,000), and anti-β-actin (1:4,000). The following secondary antibodies were used: HRP-conjugated anti-rabbit IgG (1:10,000) and HRP-conjugated anti-rabbit IgG (1:10,000). The antigens were visualized using the Clarity™ Western ECL Substrate (Bio-Rad Laboratories, Inc., Hercules, CA, USA). Blot stripping was performed using Stripping Solution (Wako Pure Chemical Industries, Ltd.). Quantification of the bands was performed using ImageJ software (National Institutes of Health, Bethesda, MD, USA).

5. Mitochondrial morphology

Cells were seeded onto 35-mm glass bottomed dishes (6.0×10^4 cells) and cultured for 3 days. In an experiment, the cells were cultured in the presence of 250 ng/ml Poly(I:C). After culturing for 3 days, the cells were stained with 100 nM MitoTracker™ Green FM (Invitrogen; Thermo Fisher Scientific, Inc.) for 30 min at 37 °C in a humidified atmosphere of 5% CO_2. After washing with medium, fresh growth medium was supplied. Fluorescence images were obtained using Olympus IX71 fluorescent microscope (Tokyo, Japan) and DP2-BSWsoftware (Olympus).

6. Quantitative reverse transcription polymerase chain Reaction (qRT-PCR)

Total RNA extraction and synthesis of complementary DNA templates were performed as previously described[21]. The synthesis of complementary DNA templates was performed using an iScript cDNA synthesis kit (Bio-Rad Laboratories, Inc.) according to the manufacturer's instructions. Quantitative RT-PCR was performed using Power SYBR® Green Master Mix (Applied Biosystems Inc., Carlsbad, CA, USA) in a Step One Plus™ system (Applied Biosystems Inc.). Differences in gene expression relative to unirradiated controls were determined using ΔCt values after normalization to the housekeeping gene *β-actin*. *β-actin* primer sequences are reported elsewhere[22]. Primer sequences for *DAP3* were 5′-AGGAGTTGCTGGGAAAGGA-3′ (sense) and 5′-TGGAAACCAGGATGGGAATA-3′ (antisense).

7. siRNA transfection

Cells were transfected with siRNA targeting *Drp1*, *Mfn1* or Control siRNA using Lipofectamine® RNAiMAX (Invitrogen; Thermo Fisher Scientific, Inc.) according to the manufacturer's protocol. Following incubation for 48 h, Drp1 and Mfn1 siRNA transfected cells were harvested and used for subsequent analyses. Transfections of siRNA targeting either *DAP3* or Control siRNA were performed twice. In brief, cells transfected for 48 h were harvested, transfected again, and cultured for another 48 h. After the second transfection, the cells were harvested and used for subsequent analyses. The final concentration of all siRNAs was 10 nM.

8. Detection of cell death

Cell death was analyzed by annexin V-FITC and PI staining as previously reported[23]. In brief, treated cells were harvested, washed, and suspended in annexin V Binding Buffer (BioLegend). Annexin V-FITC (2.5 μg/mL) and PI (50 μg/mL) solutions were added to cell suspensions and incubated for 15 min at room temperature in the dark. The cells were then analyzed using flow cytometry (Cytomics FC500; Beckman–Coulter, Fullerton, CA, USA).

9. Clonogenic survival assay

DAP3-knockdown cells were seeded onto 35-mm culture dishes (6.0×10^4 cells) and incubated for 6 h to allow them to adhere to the dish. After incubation, the cells were exposed to X-rays and cultured for about 20 h. The cultured cells were harvested using 0.1% trypsin-ethylenediaminetetraacetic acid and seeded onto 60-mm culture dishes. The cells were incubated for 7–12 days, fixed with methanol, and stained with Giemsa solution (Wako Pure Chemical Industries, Ltd.). Experiments were performed in triplicate. Colonies containing > 50 cells were counted. The surviving fraction at each radiation dose was calculated as previously reported[15].

10. Statistical analysis

Comparisons between the control and experimental groups were performed using the two-sided Student's t-test or Mann–Whitney U-test depending on data distribution. p values < 0.05 were used to indicate statistically significant differences. Excel 2016 software (Microsoft, Washington, DC, USA) along with the add-in software Statcel 4 (The Publisher OMS Ltd., Tokyo, Japan) was used to perform statistical analyses. When control group is considered as 1.0, one sample t test was performed using GraphPad QuickCalcs (https://www.graphpad.com/quickcalcs/).

Results

1. Expression of mitochondrial dynamics-related proteins and mitochondrial morphology in A549 cells treated with Poly(I:C) and/or IR

As shown in Figure 1A, the cell death in Poly(I:C)-treated A549 cells was increased with time. In addition, the effect of Poly(I:C) to increase IR-induced cell death occurred at around 48 h after cotreatment with Poly(I:C), and it was clearly observed at 72 h (Figure 1B). Therefore, to clarify the mechanisms by which Poly(I:C) modulates cellular radiation response, analyses were mainly performed at 48 or 72 h after the treatment with Poly(I:C) and/or IR in this study.

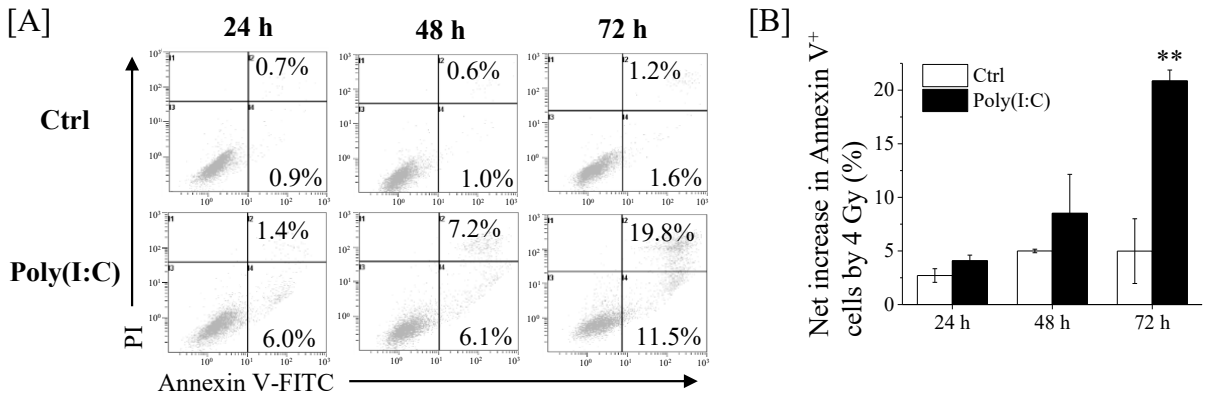

Figure 1. Effects of Poly(I:C) to induce cell death in A549 cells. (**A**) A549 cells were cultured for 24, 48 and 72 h in the presence of 250 ng/ml Poly(I:C). After culturing, the cells were harvested for cell death assay using annexin V/PI staining. Representative cytograms of annexin V/PI staining are shown. The inset numbers indicate the fractions of annexin V+/PI− or annexin V+/PI+ cells. **(B)** A549 cells were incubated with Poly(I:C). After incubation for 1 h, the cells were irradiated with 4 Gy. After culturing for 24, 48 and 72 h, the cells were harvested for cell death assay using annexin V/PI staining. The results are presented as the net increase in the fraction of annexin V+ cells (the sum of annexin V+/PI− cells and annexin V+/PI+ cells) by 4 Gy. Data are mean ± SD of three independent experiments. Symbols used: **, $p < 0.01$ versus control siRNA.

We initially analyzed the expression of mitochondrial dynamics-related proteins in A549 cells treated with Poly(I:C), IR, or both. As shown in Figure 2A and B, the expression of the mitochondria fission-related protein Drp1 was significantly lower in the cells treated with Poly(I:C) at 48 h and 72 h. Similarly, Poly(I:C) or cotreatment with Poly(I:C) and IR decreased the expression of mitochondrial fusion-related protein Mfn1 or fusion-competent long isoform OPA1 (L-OPA1), not short isoform OPA1[24], at 72 h after the treatment, whereas this was not observed at 48 h after the treatment (Figure 2A,B).

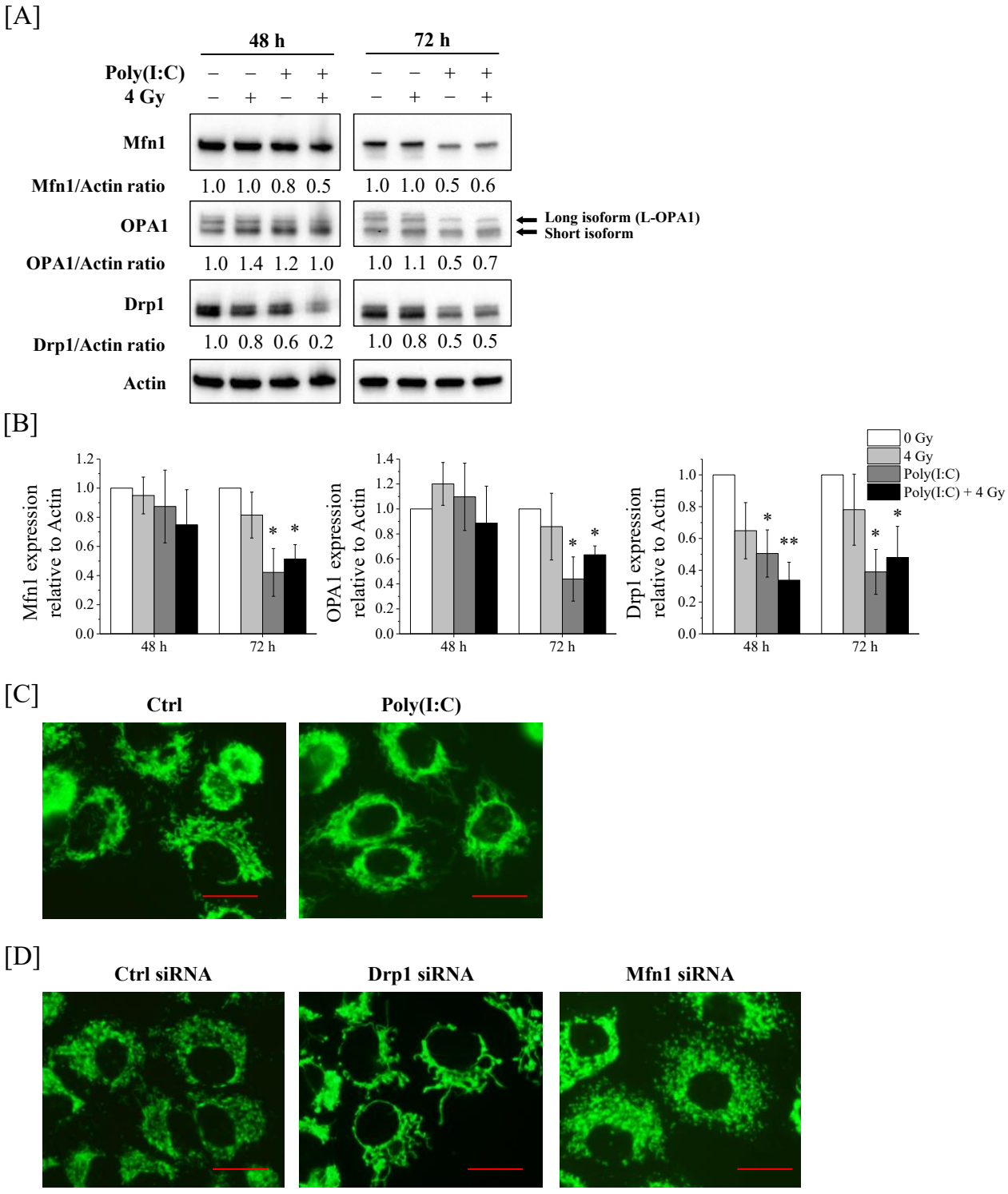

Figure 2. Effect of Poly(I:C) and/or IR on mitochondrial dynamics in A549 cells. (**A**,**B**) A549 cells were incubated with Poly(I:C). After incubation for 1 h, the cells were irradiated with 4 Gy. After culturing for 48 or 72 h, the cells were harvested for western blotting. (**A**) Representative images of immunoblots are shown. Actin was used as a loading control. (**B**) The relative values of Mfn1/actin, L-OPA1/actin and Drp1/actin ratio are presented as mean ± SD of three independent experiments. For the Drp1 proteins, both bands were quantified together. Symbols used: *, $p < 0.05$, and **, $p <$

0.01; both versus 0 Gy. (**C**) A549 cells cultured for 72 h in the presence of Poly(I:C) were harvested for mitochondrial morphology analysis using the MitoTracker™ Green FM. (**D**) A549 cells transfected with control, Drp1, or Mfn1 siRNA were cultured for 72 h and harvested for mitochondrial morphology analysis. Scale bar = 20 μM.

As Poly(I:C) decreased the expression of mitochondrial dynamics-related proteins, we analyzed the mitochondrial morphology of A549 cells treated with Poly(I:C). As shown in Figure 2C, A549 cells treated with Poly(I:C) had elongated mitochondria when compared with the control cells. This morphology was similar to that of Drp1-knockdown A549 cells wherein Drp1 protein expression was decreased by transfection with siRNA-targeting Drp1 (Figure 2D and Figure 3A) but not to Mfn1-knockdown cells whose mitochondria were fragmented (Figure 2D and Figure 4A).

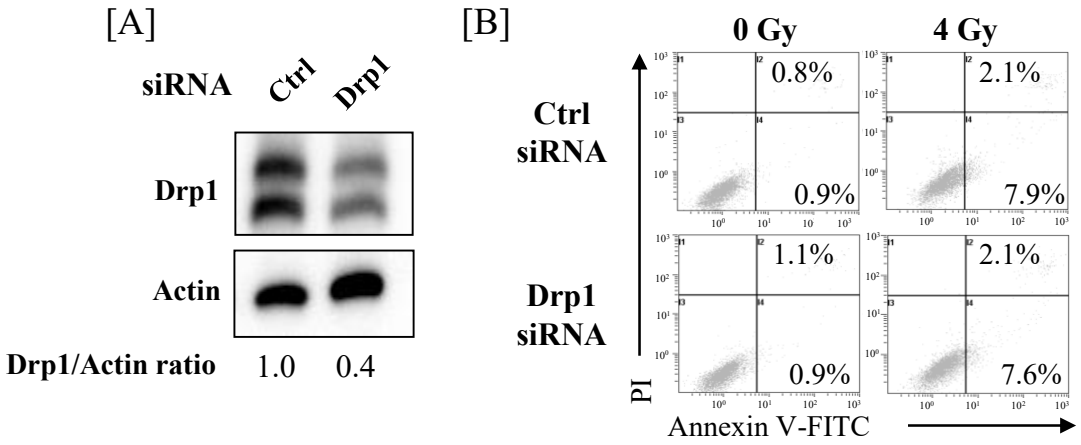

Figure 3. Effects of Drp1-knockdown on IR-induced cell death in A549 cells. (**A**) A549 cells transfected with control or Drp1 siRNA were harvested, and the Drp1 protein expression was analyzed by western blotting. Representative images of immunoblots are shown. Actin was used as a loading control. The relative values of Drp1/actin ratio are presented. For the Drp1 proteins, both bands were quantified together. (**B**) Drp1-knockdown A549 cells were treated with 4 Gy. After culturing for 72 h, the cells were harvested for cell death analysis using annexin V-FITC/PI staining. Representative cytograms of annexin V/PI staining are shown. The inset numbers indicate the fractions of annexin V+/PI− or annexin V+/PI+ cells.

2. Effect of Drp1-knockdown on IR-induced cell death in A549 cells

As Poly(I:C) decreased Drp1 expression prior to Mfn1 and L-OPA1 downregulation and as Poly(I:C)-treated A549 cells exhibited elongated mitochondria similar to that in Drp1-knockdown cells, we focused on Drp1. To investigate whether Drp1 is involved in IR-induced cell death, Drp1-knockdown A549 cells (Figure 3A) were irradiated with IR, followed by cell death analysis. Analysis of cell death

using annexin V-FITC and PI staining revealed that there was no significant difference in relative cell death (sum of annexin V+/PI− and annexin V+/PI+ cells) between control and Drp1-knockdown cells after IR (Figure 3B). Similarly, Mfn1-knockdown did not affect the IR-induced cell death in A549 cells (Figure 4B).

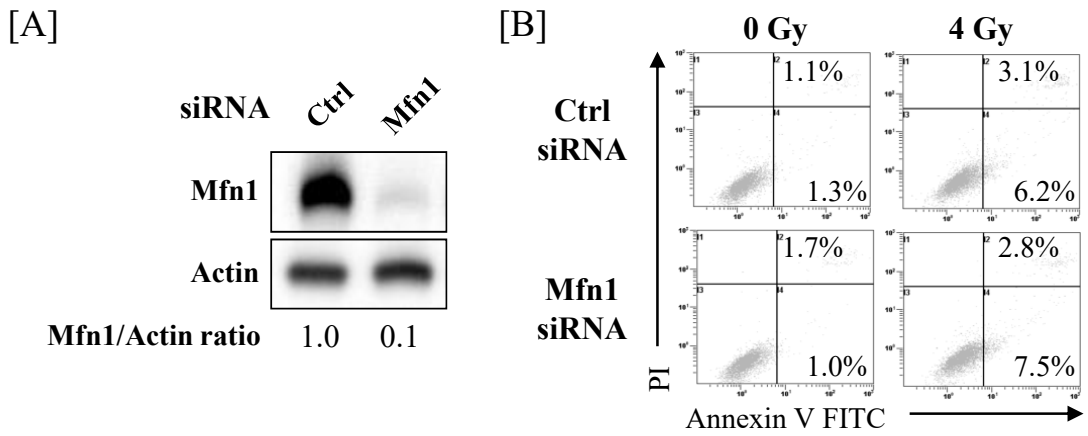

Figure 4. Effects of Mfn1-knockdown on IR-induced cell death in A549 cells. (**A**) A549 cells transfected with control or Mfn1 siRNA were harvested, and the Mfn1 protein expression was analyzed by western blotting. Representative images of immunoblots are shown. Actin was used as a loading control. The relative values of Mfn1/actin ratio are presented. (**B**) Mfn1-knockdwon A549 cells were treated with 4 Gy. After culturing for 72 h, the cells were harvested for cell death analysis using annexin V-FITC/PI staining. Representative cytograms of annexin V/PI staining are shown. The inset numbers indicate the fractions of annexin V+/PI− or annexin V+/PI+ cells.

3. Downregulation of DAP3 protein expression by Poly(I:C) in human lung adenocarcinoma cells

We then investigated DAP3 expression in A549 and H1299 human lung adenocarcinoma cells treated with Poly(I:C) and/or IR. As shown in Figure 5A, Poly(I:C) or cotreatment with Poly(I:C) and IR decreased DAP3 protein expression, and a significant decrease in DAP3 protein expression was observed in the Poly(I:C)-treated group as compared with the control group (Figure 5B).

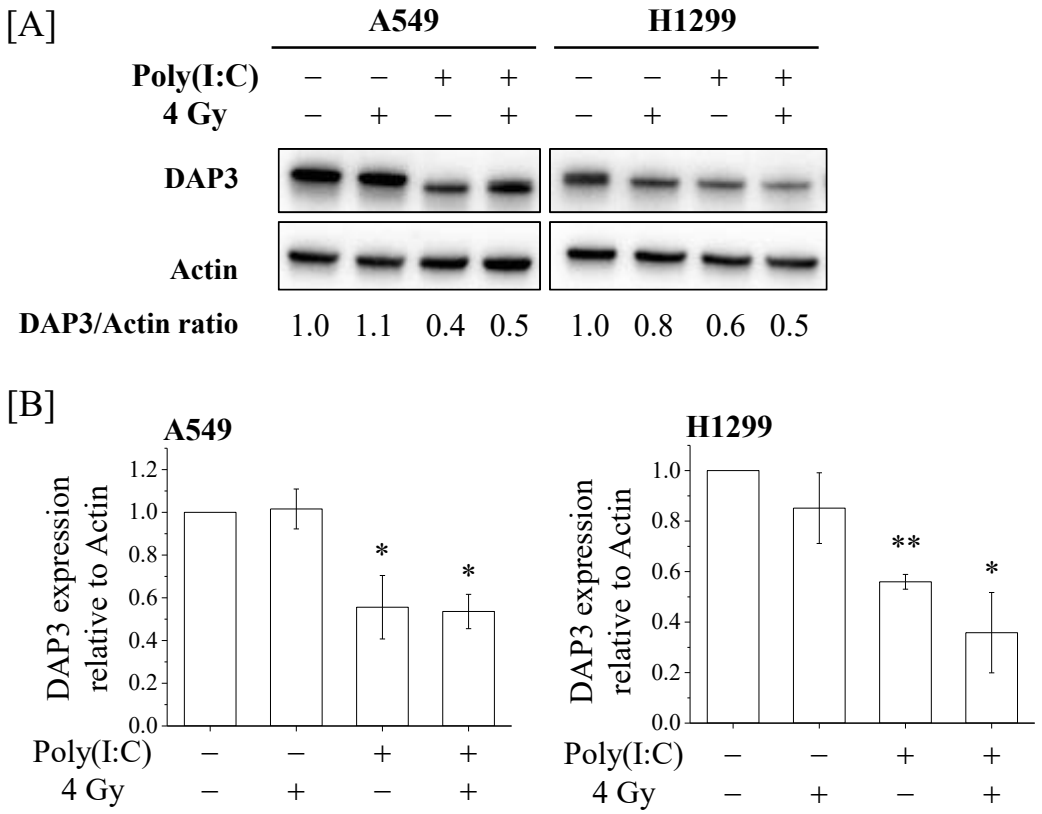

Figure 5. DAP3 expression in human lung adenocarcinoma cells treated with Poly(I:C) and/or IR. (**A**,**B**) A549 and H1299 cells were incubated with Poly(I:C). After incubation for 1 h, the cells were irradiated with 4 Gy. After culturing for 72 h, the cells were harvested for western blotting. (**A**) Representative images of immunoblots are shown. Actin was used as a loading control. (**B**) The relative values of DAP3/actin ratio are presented as mean ± SD of three independent experiments. Symbols used: *, $p < 0.05$, and **, $p < 0.01$; both versus control.

4. Involvement of DAP3 in radioresistance of human lung adenocarcinoma cells

We next examined the role of DAP3 in the radiation response of human lung adenocarcinoma cells using DAP3-knockdown cells (Figure 6A). Relative cell death in DAP3-knockdown cells following IR was higher than that in control cells (Figure 6B). Moreover, DAP3-knockdown markedly decreased the survival fraction in irradiated A549 and H1299 cells (Figure 6C). The radiation dose at

which 10% of cells survived (D_{10}) was reduced from 4.38 Gy in control cells to 2.59 Gy in DAP3-knockdown A549 cells. In H1299 cells, the D_{10} was reduced from 5.00 Gy in control cells to 3.81 Gy in DAP3-knockdown cells. Collectively, these results indicate that DAP3 is involved in radioresistance of human lung adenocarcinoma cells.

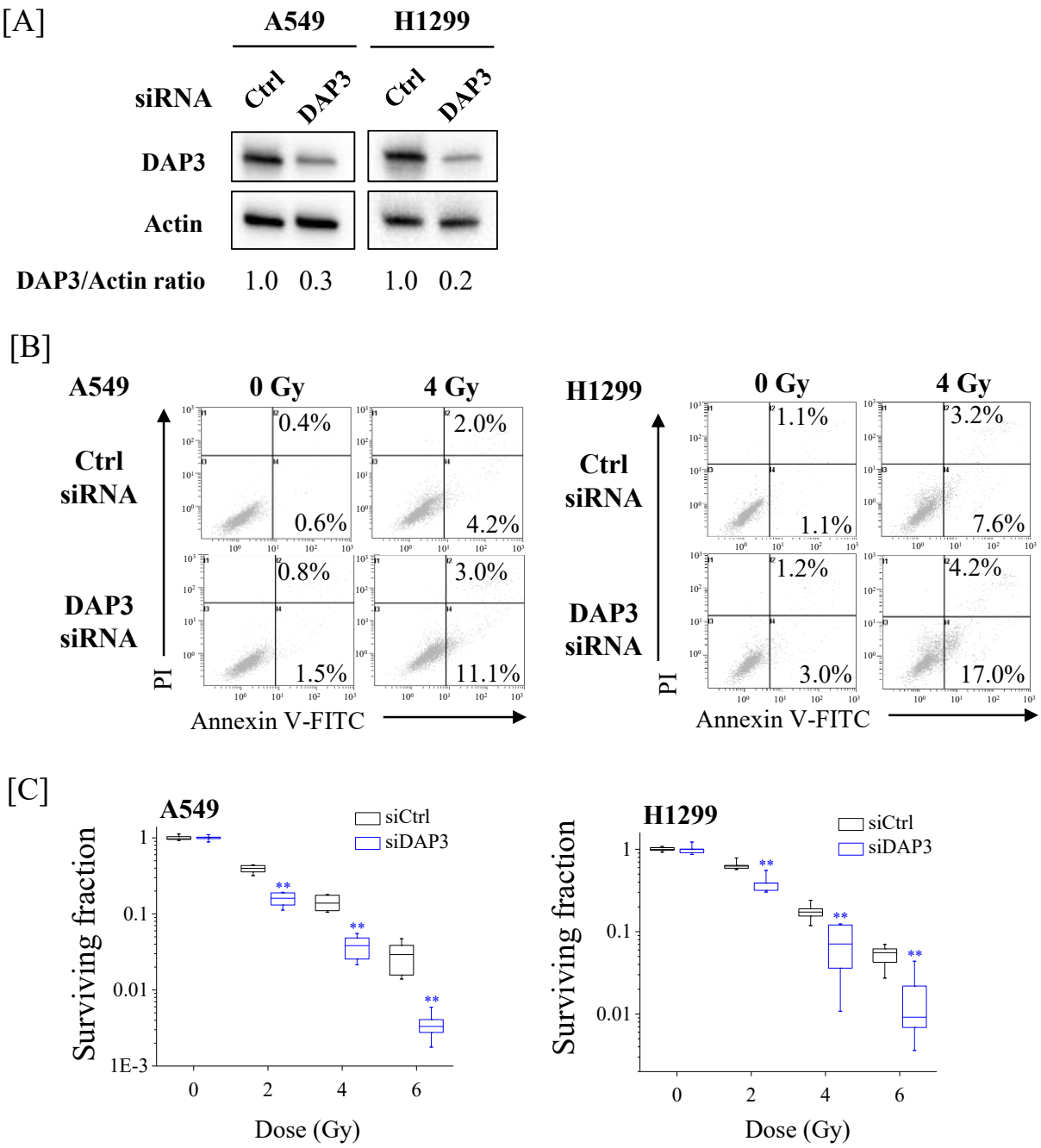

Figure 6. Effects of DAP3-knockdown on IR-induced cell death and radiosensitivity of human lung adenocarcinoma cells. (**A**) A549 and H1299 cells transfected with control or DAP3 siRNA were harvested, and DAP3 protein expression was analyzed by western blotting. Representative images of immunoblots are shown. Actin was used as a loading control. The relative values of

DAP3/actin ratio are presented. (**B**) DAP3-knockdown A549 and H1299 cells were irradiated with 4 Gy. After culturing for 72 h, the cells were harvested for cell death analysis using annexin V-FITC/PI staining. Representative cytograms of annexin V/PI staining are shown. The inset numbers indicate the fractions of annexin V+/PI− or annexin V+/PI+ cells. (**C**) DAP3-knockdown A549 and H1299 cells were irradiated with IR. After a 20-h incubation, the cells were harvested and seeded in fresh media and further cultured until noticeable growth. Box charts of the surviving fraction of A549 and H1299 cells are shown. Whiskers show minimum and maximum values, boxes represent 25–75% data ranges, horizontal lines within boxes are median. Symbols used: **, $p < 0.01$ versus control siRNA.

5. Involvement of DAP3 in the more-than-additive effect of cotreatment with Poly(I:C) and IR on cell death in human lung adenocarcinoma cells

We investigated whether DAP3 is involved in the more-than-additive increase in the death of human lung adenocarcinoma cells caused by cotreatment with Poly(I:C) and IR. In line with our recent report[15], the percentage of annexin V+ cells was higher in cotreated cells than in cells treated with IR or Poly(I:C) alone (Figure 7A(left)). The net increase in annexin V+ fraction was about 17% higher with cotreatment than the sum of fractions induced by IR and Poly(I:C) individually. Interestingly, the sum of annexin V+ fractions induced by IR and Poly(I:C) individually was increased by DAP3-knockdown, whereas no significant difference in the annexin V+ fraction of cotreated cells was observed between the control and DAP3-knockdown cells (Figure 7A(right)). As a result, the difference between that sum and the fraction of annexin V+ cells induced by cotreatment with Poly(I:C) and IR was significantly decreased to approximately 8% upon DAP3-knockdown (Figure 7A(right)). Similar to results in A549 cells, DAP3-knockdown significantly increased IR-induced cell death in H1299 cells, which diluted the more-than-additive effect of cotreatment on cell death from 8.5% to 4.2% (Figure 7B).

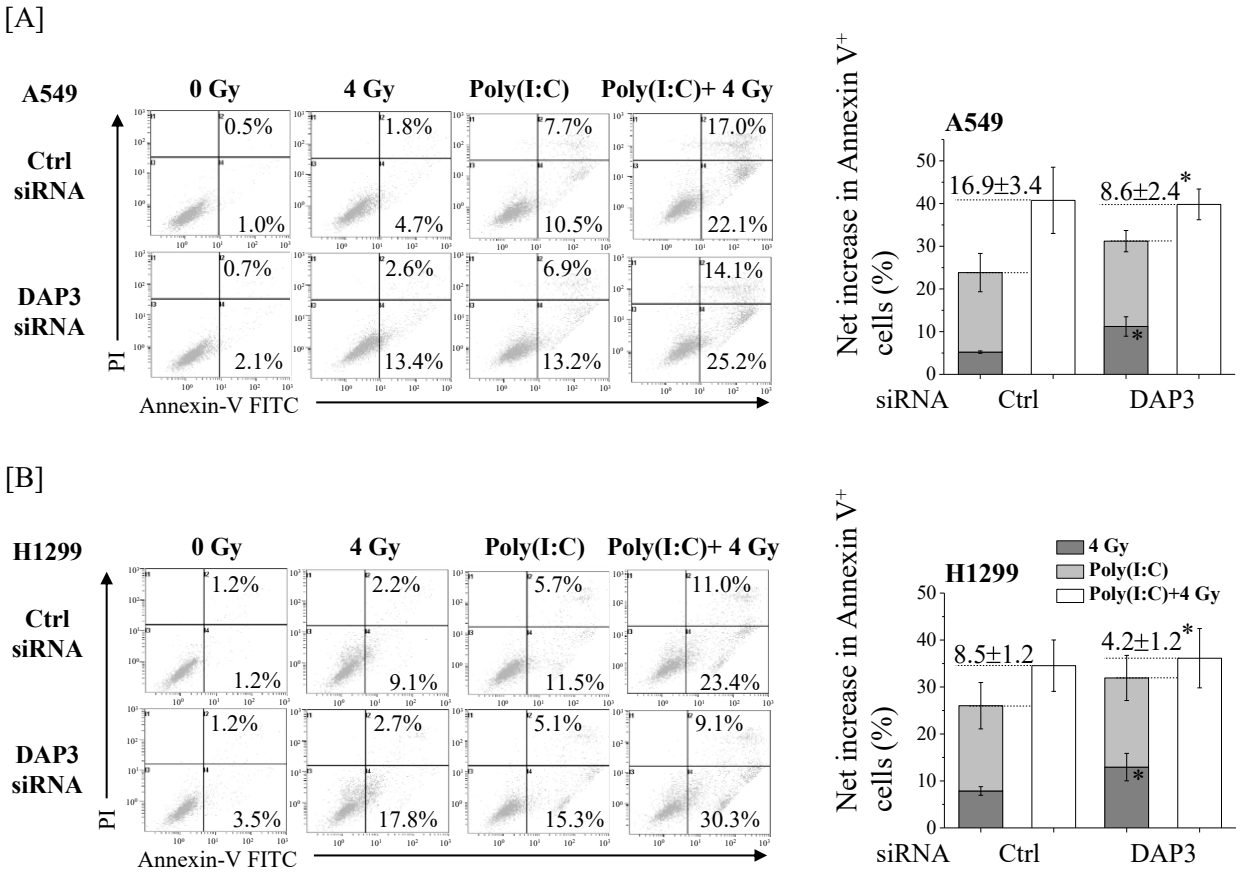

Figure 7. DAP3 is involved in the more-than-additive effect of cotreatment with Poly(I:C) and IR on induction of cell death. DAP3-knockdown A549 (**A**) and H1299 cells (**B**) were incubated with Poly(I:C). After incubation for 1 h, the cells were irradiated with 4 Gy. After culturing for 72 h, the cells were harvested for cell death assay using annexin V/PI staining. (**left**) Representative cytograms of annexin V/PI staining are shown. The inset numbers indicate the fractions of annexin V+/PI− or annexin V+/PI+ cells. (**right**) The results are presented as the net increase in the fraction of annexin V+ cells (the sum of annexin V+/PI− cells and annexin V+/PI+ cells). Data are presented as mean ± SD of three independent experiments. Symbols used: *, $p < 0.05$ versus control siRNA.

6. Post-transcriptional downregulation of DAP3 expression by Poly(I:C) in A549 cells

We finally explored the mechanism of Poly(I:C)-induced decrease in DAP3 protein expression of A549 cells. When the expression of *DAP3* mRNA in A549 cells was analyzed using quantitative reverse transcription-polymerase chain reaction (qRT-PCR), no significant difference was noted in the *DAP3* mRNA expression between the control cells and Poly(I:C)-treated cells (Figure 8A), suggesting that Poly(I:C) decreases DAP3 protein expression in a transcription-independent manner. It has been reported that double-stranded RNA induces the phosphorylation of eukaryotic initiation factor-2α (eIF-2α), which inhibits the translation of mRNA[25]. Therefore, we analyzed the effect of

Poly(I:C) on the expression of phosphorylated eIF-2α (p-eIF-2α). As shown in Figure 8B,C, Poly(I:C) increased p-eIF-2α expression, followed by the downregulation of DAP3 protein expression.

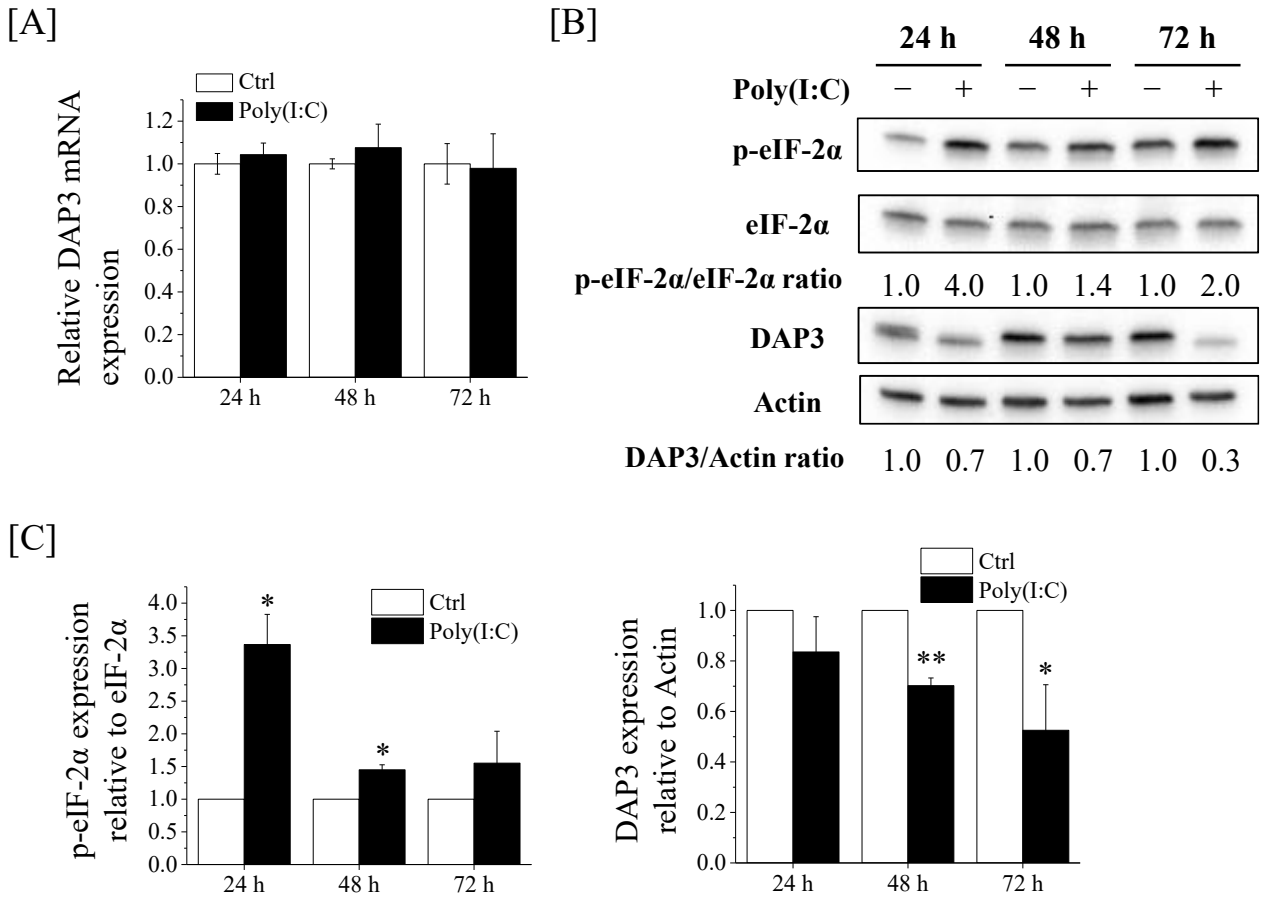

Figure 8. Effects of Poly(I:C) on the *DAP3* mRNA expression and p-eIF-2α protein expression in A549 cells. (**A**) A549 cells were cultured with Poly(I:C) for 24–72 h and harvested for qRT-PCR. Data are presented as mean ± SD of three independent experiments. (**B**,**C**) A549 cells treated with Poly(I:C) were cultured for 24–72 h and harvested for western blotting. (**B**) Representative images of immunoblots are shown. Actin was used as the loading control. (**C**) The relative values of phosphorylated eukaryotic initiation factor-2α (p-eIF-2α)/eIF-2α and DAP3/actin ratio are presented as mean ± SD of three independent experiments. Symbols used: *, $p < 0.05$, and **, $p < 0.01$; both versus control.

Discussion

RLRs elicit immune responses against viruses and tumors through the mitochondria[26,27]. We previously reported that the RLR agonist Poly(I:C) enhanced radiosensitivity and that cotreatment with Poly(I:C) and IR more than additively increased cell death in human lung adenocarcinoma cells[15]. However, it remains unknown how Poly(I:C) modulates the cellular radiation response in human lung adenocarcinoma cells. Here we investigated the involvement of mitochondrial dynamics and the mitochondrial ribosome protein DAP3 in the modulation of the cellular radiation response by Poly(I:C). The present results demonstrate that Poly(I:C) decreased mitochondrial dynamics-related proteins and DAP3 protein expression. However, siRNA experiments revealed that DAP3, but not mitochondrial dynamics, regulates radioresistance and is involved in the more-than-additive effect of cotreatment with Poly(I:C) and IR on cell death in human lung adenocarcinoma cells.

Several studies have reported the relationship between mitochondrial dynamics and viral infection or RLR-mediated antiviral pathway[5,28-30]. For example, it has been reported that RLR activation induces the elongation of mitochondria[5]. In addition, dengue and human immunodeficiency viruses, which are detected by RLR[31,32], promote mitochondrial fusion by decreasing Drp1 expression[29,30]. These findings support our observations that Poly(I:C) reduces the Drp1 expression and induces mitochondrial elongation. Intriguingly, we observed a decrease in Mfn1 and L-OPA1 expressions following the downregulation of the Drp1 expression (Figure 2A,B). Saita et al. reported that the knockdown of Drp1 promotes the degradation of Mfn1 and L-OPA1 protein expression via the ubiquitin–proteosome systems and proteolytic cleavage, respectively[33]. Therefore, it is likely that the decrease in Mfn1 and L-OPA1 protein expressions resulted from the downregulation of Drp1 expression by Poly(I:C).

Although some reports indicate the involvement of Drp1 in cell death[16,34-36], this was not observed in A549 cells in this study. For example, Kobashigawa et al. reported that normal human fibroblast cells with Drp1-knockdown were resistant to gamma irradiation[34]. Similarly, Xu et al. showed that arenobufagin- or staurosporine-induced cell death was decreased by Drp1-knockdown in HCT116 human colon cancer cells[35]. These reports indicate that Drp1 mediates cell death. Conversely, the protective effects of Drp1 on cell death have also been reported[37-39]. For example, depletion of Drp1 is known to increase apoptosis in human colon cancer cells[37]. In addition, Chen et al. reported that silencing of Drp1 increased radiosensitivity of UM87MG and T98G human glioblastoma cells[38]. Furthermore, Akita et al. demonstrated that Drp1-knockdown sensitized A375 cells (a human malignant melanoma) and A549 to tumor necrosis factor-related apoptosis-inducing ligand, although Drp1-knockdown by itself did not increase the rate of apoptosis[39]. Therefore, taken together, it is likely that the involvement of Drp1 in cell death depends on the types of cell and

stimulus-inducing cell death.

A pro-apoptotic effect of DAP3 has been reported[40-42]. DAP3 was originally identified as a mediator of IFN-gamma-induced cell death by functional gene cloning[40]. In addition, Miyazaki et al. showed that DAP3 expression was required for inducting anoikis, which is programmed cell death caused by loss of adhesion[41]. In contrast to these reports, Henning[19] and the current study suggest that DAP3 is related to radioresistance. Therefore, the role of DAP3 in cell death may depend on the type of stimulus inducing cell death.

Although this study depicted the involvement of DAP3 in radioresistance of human lung adenocarcinoma cells, the mechanism by which DAP3 regulates radioresistance remains unclear. DAP3 is known to control the mitochondria dynamics as well as the mitochondrial function. Xiao et al. reported that the knockdown of DAP3 increased the fragmentation in mitochondria[43]. We also observed fragmented mitochondria in DAP3-knockdown A549 cells (data not shown). Since several reports have demonstrated an association between mitochondria fission and cell death[16,34-36,44,45], we assumed that mitochondrial fragmentation contributes to the increase in IR-induced cell death via DAP3-knockdown. However, Mfn1-knockdown leading to mitochondrial fragmentation did not affect the IR-induced cell death in A549 cells (Figure 2D and Figure 4). Therefore, it is likely that DAP3 controls the radioresistance of lung adenocarcinoma cells in a mitochondria fission-independent manner. Mitochondrial functions, such as energy metabolism, are closely related to the radioresistance of most cancers, including lung cancer[46,47]. Since DAP3 is essential for maintaining mitochondrial functions, including ATP production[43], it is possible that DAP3-knockdown causes radiosensitization through impairment of mitochondrial functions, such as energy metabolism. Further studies focusing on mitochondrial function are needed to clarify DAP3-mediated radioresistance mechanisms.

As mentioned earlier, the fragmentation of mitochondria was observed in DAP3-knockdown A549 cells (data not shown). Interestingly, Poly(I:C) treatment induced mitochondrial elongation despite the downregulation of DAP3 protein expression (Figure 2C). Xiao et al. reported that DAP3-knockdown increased the fragmentation of mitochondrial through phosphorylation of Drp1[43]. Considering that Poly(I:C) reduces not only DAP3 but also Drp1 protein expression and that the mitochondria morphology of Poly(I:C)-treated cells is similar to that of Drp1-knockdown cells, it seems that the mitochondrial morphology of Poly(I:C)-treated A549 cells is predominantly regulated by the downregulation of the Drp1 expression.

Here, we showed that DAP3-knockdown increased cell death after IR (Figure 6). Notably, DAP3-knockdown did not affect the cell death induced by cotreatment with Poly(I:C) and IR (Figure 7). These results suggest that the effect of Poly(I:C) to increase IR-induced cell death is related to DAP3, because if the effect is independent of DAP3, DAP3-knockdown should further increase cell

death induced by cotreatment with Poly(I:C) and IR. Since Poly(I:C) decreased DAP3 protein expression, it is believed that Poly(I:C) increases IR-induced cell death through the downregulation of DAP3 expression.

The present results suggest that downregulation of DAP3 protein expression by Poly(I:C) participated in the more-than-additive effect of cotreatment on cell death. To the best of our knowledge, this is the first study to suggest that an RLR agonist negatively regulates DAP3 protein expression. Interestingly, Poly(I:C) post-transcriptionally decreased DAP3 protein expression (Figure 8). Since Poly(I:C) increased the p-eIF-2α expression followed by the downregulation of DAP3 protein expression, it is believed that Poly(I:C) decreased DAP3 protein expression through inhibition of translation of *DAP3* mRNA. Indeed, we could not exclude the possibility that mtDNA was involved in the post-transcriptional regulation of DAP3 expression by Poly(I:C). A previous report suggests that the amount of mtDNA controls DAP3 protein expression[48] and that infection with human immunodeficiency virus 1, which is detected by RLR[31], decreases mtDNA[49]. Further study of mtDNA will be required to investigate this possibility.

In conclusion, we show that the downregulation of DAP3 protein expression by Poly(I:C) contributes to the more-than-additive effect of cotreatment with Poly(I:C) and IR on cell death in human lung adenocarcinoma cells. In addition, the present results highlighting the importance of DAP3 in the cellular radiation response of human lung adenocarcinoma cells improve our understanding of DAP3-mediated radioresistance mechanisms and have implications on the efficacy of radiation therapy for lung adenocarcinoma.

Chapter 2. DAP3-mediated cell cycle regulation and its association with radioresistance in human lung adenocarcinoma cell lines

Introduction

Lung cancer is the leading cause of cancer-related deaths worldwide[50]. Non-small cell lung cancer accounts for 85% of lung cancer cases, of which lung adenocarcinoma (LUAD) is the largest subgroup[51]. Lung cancer can be treated through the use of chemotherapy, radiotherapy, and surgery. However, the efficiency of radiotherapy can be stalled by radioresistance, thereby resulting in a reduced treatment success[52]. Hence, more light must be shed on the molecular mechanisms underlying the radioresistance of LUAD.

Mitochondria are cellular organelles responsible for energy conversion and adenosine triphosphate (ATP) production in eukaryotic cells. Mitochondria have their own genome as well as a specific protein synthesis machinery served by the mitochondrial ribosomes. In addition to the ribosomal function, some of the mitochondrial ribosomal proteins are known to participant in the other cellular functions[53-55]. For example, mitochondrial ribosomal protein L41 has been reported to block the anti-apoptotic activity of Bcl-2 and to induce caspase-mediated apoptosis[54]. In addition, Wang et al. have reported that mitochondrial ribosomal protein S16 promote glioma cell growth, migration and invasion by the activating phosphatidylinositol-3 kinase/AKT/Snail axis[55]. In terms of mitochondrial ribosomal protein S29 (death-associated protein 3, DAP3), Henning has reported that the overexpression DAP3 can confer radioresistance to ataxia-telangiectasia cells exhibiting high radiosensitivity[19]. We have also reported that DAP3 is involved in the radioresistance of human LUAD cell lines[56], though it remains unclear how DAP3 can modulate the radioresistance.

Ionizing radiation is known to cause cytotoxicity through DNA damage. In irradiated cells, cell cycle progression is transiently arrested for the undertaking of DNA repair through the activation of checkpoint kinases, thereby resulting in radioresistance[57,58]. Ionizing radiation is known to activate checkpoint kinase 1 (chk1) and lead to cell cycle G2/M arrest through the inactivation of cyclin B1 and the cdc2 complex, while chk2 activation leads to a cell cycle G1 arrest through p53 [58,59].

It has also been reported that some proteins involved in resistance to chemotherapy and radiotherapy actually regulate the cell cycle arrest[60,61]. For example, Huang et al. have reported that the Ras-associated binding protein Rab12 mRNA and protein expressions are upregulated in cervical cancer tissues, and that Rab12 promotes radioresistance by inducing a G2/M arrest[61] . Therefore, we have hypothesized that DAP3 can regulate radioresistance through a cell cycle regulation. However, to date, there have been no reports regarding this issue. Therefore, the present study has investigated our hypothesis that DAP3 regulates radioresistance through radiation-induced cell cycle arrest in human LUAD cell lines.

Materials & Methods

1. Reagents

Calcium^{2+} and magnesium^{2+} free phosphate-buffered saline (PBS) and paclitaxel (cat. no. 169-18611) were purchased from Wako Pure Chemical Industries, Ltd. (Osaka, Japan). Propidium iodide (PI) and the chk2 inhibitor II were purchased from Sigma-Aldrich (Merck KGaA, Darmstadt, Germany). SCH900776 was purchased from Med Chem Express (Shanghai, China). The anti-rabbit horseradish peroxidase (HRP)-conjugated IgG (cat. no. 7074), and the anti-mouse HRP-conjugated IgG (cat. no. 7076) secondary antibodies, as well as the anti-phospho-cdc2 (Tyr15) (cat. no. 9111), the anti-cyclin B1 (cat. no. 4135), the anti-phospho-histone H3 (Ser10) XP (cat. no. 3377), the anti-phospho-chk1 (Ser296) (cat. no. 2349), the anti-phospho-chk2 (Thr68) (cat. no. 2661), the anti-p21 (cat. no. 2947), and the anti-β-actin (cat. no. 4967) monoclonal antibodies were purchased from Cell Signaling Technology Inc. (Danvers, MA, USA). The anti-DAP3 (cat. no. 610662) monoclonal primary antibody was purchased from BD Biosciences (Franklin Lakes, NJ, USA). The Ambion Silencer® Select Pre-designed siRNA against the gene-encoding DAP3 (cat. no. s1506), and the Silencer® Select Negative #1 Control (cat. no. AM4611) siRNAs were purchased from Thermo Fisher Scientific, Inc. (Waltham, MA, USA).

2. Cell culture and treatment

Human LUAD A549 and H1299 cells were purchased from the Riken Bio-Resource Center (Tsukuba, Japan) and the American Type Culture Collection (Manassas, VA, USA), respectively. A549 cells were maintained in Dulbecco's modified Eagle's medium (Sigma-Aldrich) supplemented with 10% heat-inactivated fetal bovine serum (FBS; Sigma-Aldrich) and 1% penicillin/streptomycin (Wako Pure Chemical Industries, Ltd), at 37°C, in a humidified atmosphere of 5% CO_2. H1299 cells were maintained in RPMI 1640 medium (Gibco®; Invitrogen/Thermo Fisher Scientific, Waltham, MA, USA) supplemented with 10% FBS and 1% penicillin/streptomycin, at 37°C, in a humidified atmosphere of 5% CO_2.

Cells were seeded onto 35-mm culture dishes (6.0×10^4 cells) or 60-mm culture dishes (1.2×10^5 cells) (Sumitomo Bakelite Co., Ltd, Tokyo, Japan) and were cultured overnight so as to allow them to adhere to the dish. Subsequently, the cells were harvested by using 0.1% trypsin-ethylenediaminetetraacetic acid (Wako Pure Chemical Industries, Ltd), and the number of viable cells was counted by using a trypan blue dye exclusion assay before any subsequent analysis was undertaken. In experiments using checkpoint kinase inhibitors, we used SCH900776 as a chk1 inhibitor [62], and chk2 inhibitor II as a chk2 inhibitor[63]. In fact, chk1 (400 nM) and/or chk2 (10 μM) inhibitors were added to the culture medium just 1 h before the irradiation.

3. In vitro X-ray irradiation

Cells were irradiated (150 kVp; 20 mA; 0.5-mm Al filter and 0.3-mm Cu filter) by using an X-ray generator (MBR-1520R-3; Hitachi, Ltd., Tokyo, Japan) at a distance of 450 mm from the focus and at a dose rate of 1.00–1.03 Gy/min.

4. siRNA transfection

Transfections of siRNA targeting either DAP3 or the control siRNA were performed twice by using Lipofectamine® RNAiMAX (Invitrogen; Thermo Fisher Scientific, Inc.) according to the manufacturer's protocol. In brief, cells transfected for 48 h were harvested, transfected again, and cultured for another 48 h. After the second transfection, the cells were harvested and used for the undertaking of subsequent analyses. The final concentration of all siRNAs was 10 nM.

5. Cell cycle analysis

Cell cycle analysis was performed, as previously described[64]. Harvested cells were fixed overnight in ice-cold 70% ethanol at −20°C. Fixed cells were washed with and subsequently suspended in PBS(−), and they were treated with 20 μg/mL RNase A for 30 min, at 37°C. Following this treatment, the cells were resuspended in PBS(−) containing 20 μg/mL PI, and were incubated in the dark for 30 min. Finally, the cells were passed through a cell strainer (BD Falcon; BD Biosciences, Franklin Lakes, NJ, USA) and were analyzed by using a flow cytometer (Cytomics FC500; Beckman–Coulter, Fullerton, CA, USA).

6. SDS-PAGE and western blotting

SDS-PAGE and Western blotting analysis were performed as previously reported[17]. The following primary antibodies were used: anti-phospho-cdc2 (1:3,000), anti-cyclin B1 (1:3,000), anti-phospho-histone H3 (1:3,000), anti-cyclin B1 (1:3,000), anti-phospho-chk1 (1:3,000), anti-chk1 (1:3,000), anti-phospho-chk2 (1:3,000), anti-chk2 (1:3,000), anti-DAP3 (1:3,000), anti-cyclin D1 (1:3,000), anti-p21 (1:3,000), anti-GAPDH (1:4,000), and anti-β-actin (1:4,000). The following secondary antibodies were used: HRP-conjugated anti-rabbit IgG (1:10,000) and HRP-conjugated anti-rabbit IgG (1:10,000). The antigens were visualized by using the Clarity MAX™ Western ECL Substrate (Bio-Rad Laboratories, Inc., Hercules, CA, USA) for phosphor-chk2 or the Clarity™ Western ECL Substrate (Bio-Rad Laboratories, Inc.) for the other proteins. Blot stripping was performed by using Stripping Solution (Wako Pure Chemical Industries, Ltd). Images for proteins other than p21 were captured by using the Cool Saver AE-6955 (ATTO, Tokyo, Japan), while the images of p21 were captured by using the iBright 1500 Imaging System (Invitrogen; Thermo Fisher Scientific, Inc.). The

quantification of the bands was performed by using the ImageJ software (National Institutes of Health, Bethesda, MD, USA).

7. Mitotic catastrophe analysis

The cells on coverslips were incubated under the indicated conditions, were fixed for 10 min in 4% paraformaldehyde in PBS(−), and were then permeabilized with 1% Triton X-100 in PBS(−) for 10 min, at room temperature. In order to prepare the cells arrested in mitosis, paclitaxel (10 μM) was added to the culture medium. After 24 h, the cells were harvested for the undertaking of the subsequent analysis. The samples were mounted onto coverslips by using Vectashield® Mounting Medium with DAPI (Vector Laboratories, Inc., Burlingame, CA, USA), and were examined by using an Olympus IX71 fluorescent microscope (Tokyo, Japan) and the DP2-BSWsoftware (Olympus). At least 100 cells were analyzed.

8. Clonogenic survival assay

Cells were seeded onto 35-mm culture dishes (6.0×10^4 cells) and were incubated overnight. After incubation, the cells were exposed to X-rays and were further incubated for 24 h. The cultured cells were harvested by using 0.1% trypsin-ethylenediaminetetraacetic acid, and were seeded onto 60-mm culture dishes. The cells were further incubated for 7–8 days, were fixed with methanol, and were stained with Giemsa solution (Wako Pure Chemical Industries, Ltd). Experiments were performed in triplicate. Colonies containing >50 cells were counted. The surviving fraction at each radiation dose was calculated as previously described in detail[20].

9. Bioinformatics and data analysis

DAP3 expression in tumor and non-tumor tissue samples was downloaded from Cancer RNA-Seq Nexus (http://syslab4.nchu.edu.tw/) and reanalyzed. mRNA levels of *DAP3* and the overall survival of human LUAD patients in the The Cancer Genome Atlas (TCGA) cohort was analyzed through cBioportal for Cancer Genomics (https://www.cbioportal.org/). The patients whose *DAP3* mRNA expression z-scores (RNA-Seq V2 RSEM) were greater than 0.5 SD above mean, were defined as "DAP3 high" patients.

10. Statistical analysis

Data are presented as the mean ± standard deviation (SD) of three independent experiments. Comparisons between the control and experimental groups were performed by using the two-sided Student's *t*-test. Values of p found to be < 0.05 were considered as indicative of statistically significant differences. The Excel 2016 software (Microsoft, Washington, DC, USA) and the add-in

software Statcel 4 (The Publisher OMS Ltd, Tokyo, Japan) were used in order to perform the required statistical analyses. When the control group was considered as 1.0, one sample *t*-test was performed by using GraphPad QuickCalcs (https://www.graphpad.com/quickcalcs/).

Results

1. Involvement of DAP3 in radiation-induced G2/M arrest

We initially investigated the cell cycle distribution of DAP3-knockdown A549 and H1299 cells (Figure 1A). As shown in Figure 1B, although the DAP3 knockdown hardly affected the cell cycle distribution of non-irradiated A549 cells, it did attenuate the increase in G2/M population at 8 h after irradiation. Similar results were observed in H1299 cells (Figure 1C). These results suggest that DAP3 is involved in the radiation-induced G2/M arrest in human LUAD cell lines.

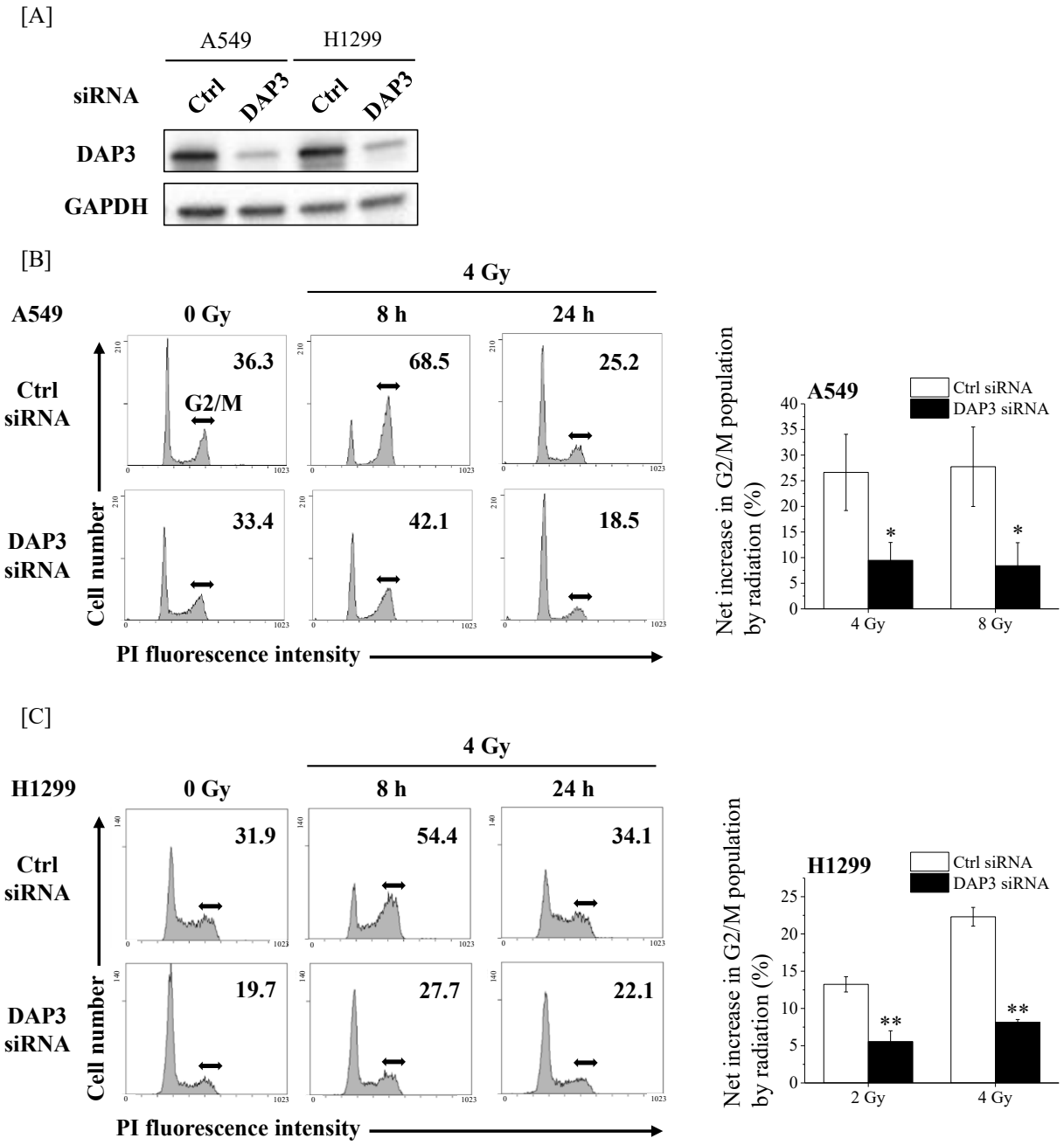

Figure 1. Involvement of DAP3 in the radiation-induced G2/M arrest of human LUAD cell lines. (**A**) Human LUAD cell lines (A549 and H1299) transfected with control or DAP3 siRNA were harvested, and the DAP3 protein expression was analyzed through Western blotting. A representative image of an immunoblot is shown. GAPDH was used as the loading control. (**B,C**) Human LUAD cell lines transfected with control or DAP3 siRNA were harvested and treated with radiation. After 8 or 24 h of culturing, the cells were harvested for cell cycle analysis. (**Left**) Representative histograms and the obtained data are presented. Double-headed arrows indicate the G2/M population, while the inset number in the figure indicates the G2/M proportion in the total cells. (**Right**) The net increase in G2/M populations as a result of the undertaken irradiation is shown. Symbols used: *, $p < 0.05$, and **, $p < 0.01$; both versus control siRNA.

2. Enhancement of radiation-induced mitotic catastrophe by DAP3 knockdown

Since the aberrant cell cycle checkpoints usually result in mitotic catastrophe, which is a form of radiation-induced cell death[65-67], we subsequently examined the effect of DAP3 knockdown on radiation-induced mitotic catastrophe. In order to identify mitotic catastrophe, the cells were analyzed for the presence of micronuclei, multi-lobular nuclei, and fragmented nuclei (Figure 2A). As shown in Figure 2B, DAP3 knockdown hardly increased the percentage of mitotic catastrophe in non-irradiated cells. As expected, the percentage of mitotic catastrophe was significantly higher in DAP3-knockdown irradiated cells than that in control irradiated cells.

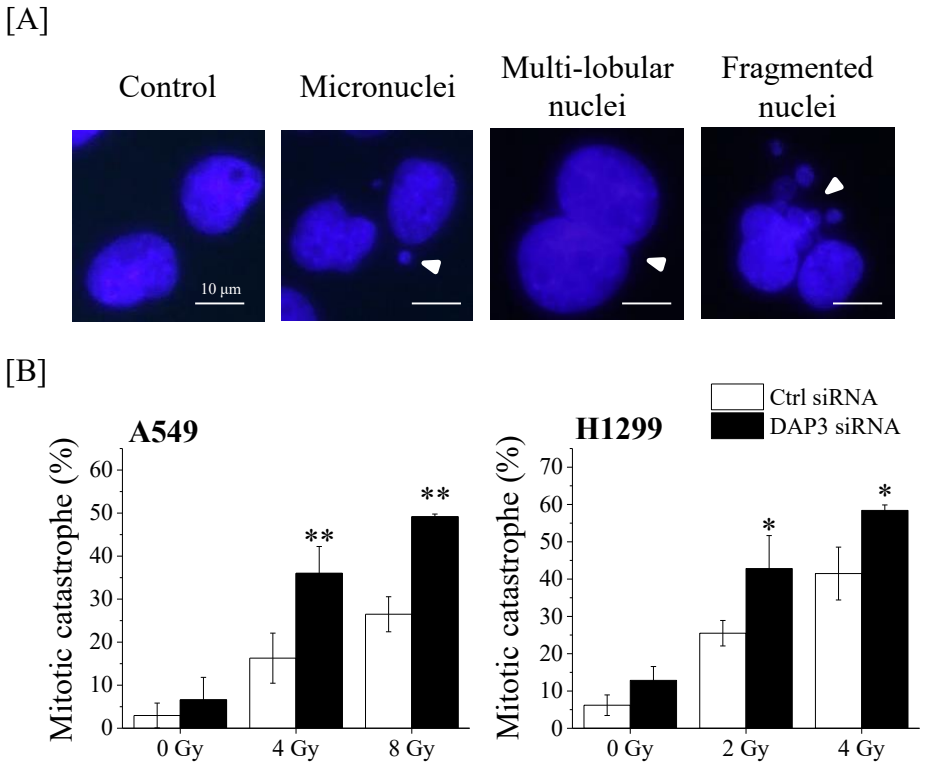

Figure 2. Effect of DAP3 knockdown on radiation-induced mitotic catastrophe in human LUAD cell lines. (**A,B**) Human LUAD cell lines transfected with control or DAP3 siRNA were treated with radiation. After 72 h of culturing, the cells were harvested for the analysis of mitotic catastrophe. (**Top**) Representative pictures of mitotic catastrophe are shown. Micronuclei, multilobed nuclei, and fragmented nuclei were counted as indicative of the occurring mitotic catastrophe. Arrows indicate the cells undergoing mitotic catastrophe. (**B**) The percentages of the cells affected by mitotic catastrophe are shown. Symbols used: *, $p < 0.05$, and **, $p < 0.01$; both versus control siRNA.

3. Reduction of radiation-induced expressions of proteins related to G2/M arrest by DAP3 knockdown

In an attempt to elucidate the role of DAP3 in radiation-induced G2/M arrest, we firstly investigated whether the radiation-induced G2/M arrest is a G2- or an M-phase arrest through the study of the expression of phosphorylated-histone H3 (pH3), which is known to be upregulated in mitotic cells. We used paclitaxel-treated A549 cells as a positive control for M-phase cells where an upregulation of the pH3 expression was evident (Figure 3), whereas a lower expression of pH3 was observed in radiation-induced G2/M arrested A549 cells, and DAP3 knockdown hardly affected the pH3 expression in irradiated cells (Figure 3). These findings indicate that the cell cycle arrest occurred at the G2 phase (rather than the M-phase) in the irradiated cells, and that DAP3 regulates the radiation-induced G2 arrest in human LUAD cell lines.

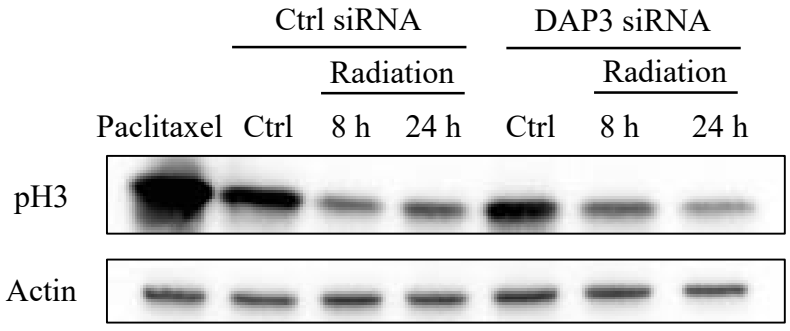

Figure 3. Effect of radiation on the expression of the M-phase marker phosphorylated-histone H3. A549 cells cultured for 24 h in the presence of DMSO or paclitaxel, or A549 cells transfected with control or DAP3 siRNA, were treated with radiation and were subsequently cultured for 8 or 24 h. The cells were harvested for the undertaking of Western blot analysis. A representative image of an immunoblot is shown. Actin was used as the loading control, while pH3 indicates the phosphorylated-histone H3.

Therefore, we then investigated the effect of the DAP3 knockdown on the expression of key regulators of the G2 arrest. The latter is known to be accompanied by an upregulation of cyclin

B1 and a phosphorylation of cdc2 (pcdc2) [58,59]. Figure 4A shows that the expressions of cyclin B1 and pcdc2 were increased in the irradiated A549 cells, and that the DAP3 knockdown decreased the radiation-induced increase of the pcdc2 expression. In H1299 cells, DAP3 knockdown attenuated the steady level as well as the radiation-induced expression of both cyclin B1 and pcdc2 (Figure 4B).

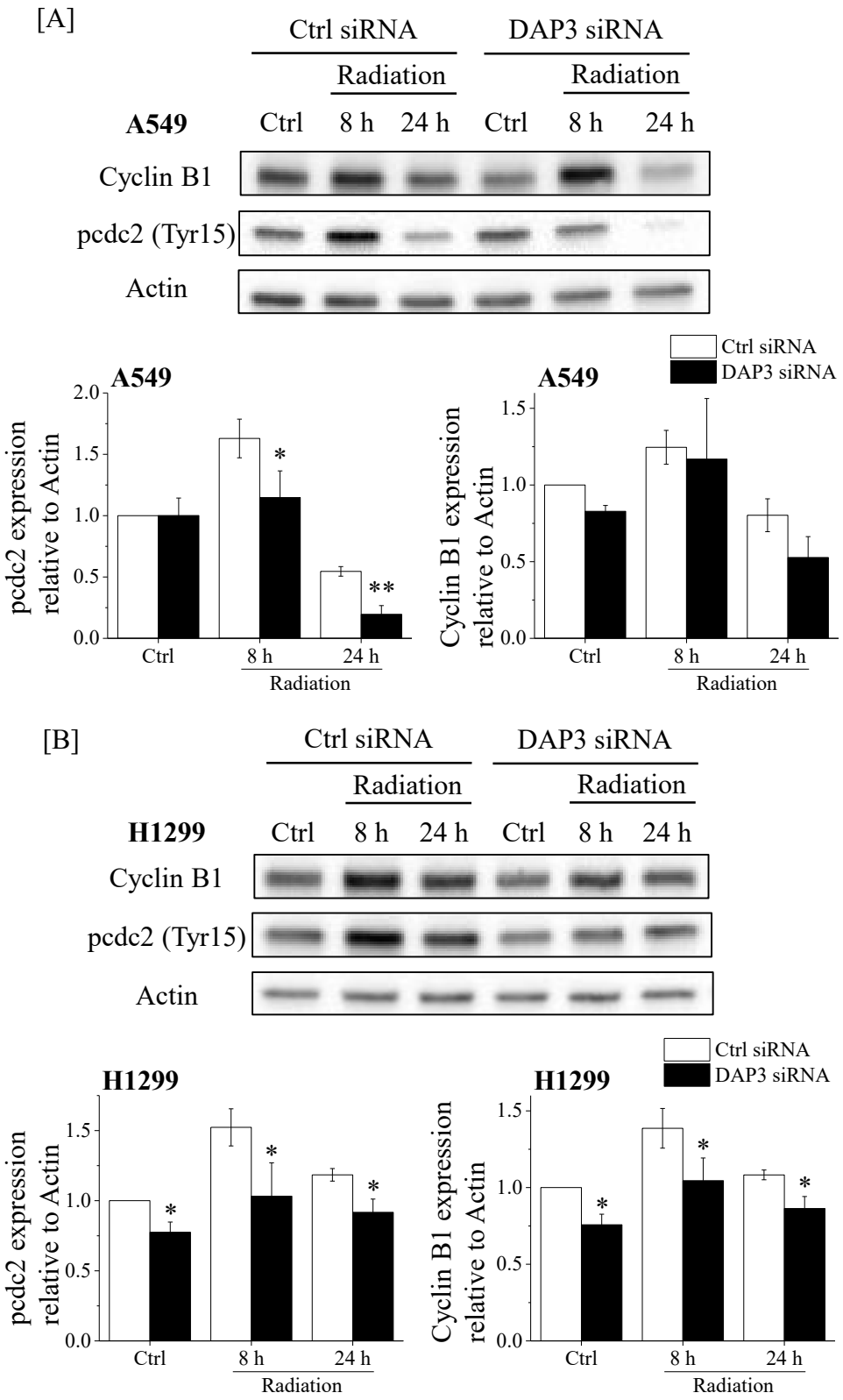

Figure 4. Effects of DAP3 knockdown on the expression of G2 arrest regulators in irradiated human LUAD cell lines. (**A,B**) A549 (**A**) and H1299 (**B**) cells transfected with control or DAP3 siRNA were treated with 4-Gy irradiation, and were cultured for 8 or 24 h. The cells were harvested for the undertaking of Western blot analysis. A representative image of an immunoblot is shown. Actin was used as the loading control. The relative values of the pcdc2/actin and the cyclin B1/actin ratios are presented, where pcdc2 indicates the phosphorylated-cdc2. Symbols used: *, $p < 0.05$, and **, $p < 0.01$; both versus control siRNA.

4. Involvement of DAP3 in radiation-induced phosphorylated expressions of checkpoint kinases

In order to further characterize the underlying mechanism of the DAP3-mediated radiation-induced G2 arrest, we investigated the effect of DAP3 knockdown on the expression of chk1 and of chk2, which are regulators of cdc2 and cyclin B1[58,59]. As shown in Figure 5A, the pchk1/actin and the pchk2/actin ratios were increased at 0.5 h after the irradiation. Interestingly, the DAP3 knockdown significantly suppressed the increase in the pchk1/actin ratio, and partially suppressed the pchk2/actin ratio in irradiated cells (Figure 5A). Similar results were observed in H1299 cells (Figure 5B).

5. Involvement of chk1 in radiation-induced G2 arrest

Since the DAP3 knockdown decreased the radiation-induced pchk1 expression in both A549 and H1299 cells (Figure 5), we subsequently examined the role of chk1 on the radiation-induced G2 arrest in human LUAD cell lines by using the chk1 inhibitor. As shown in Figure 6A, similarly to the DAP3 knockdown, chk1 inhibitor decreased the radiation-induced G2/M population in human LUAD cell lines. In contrast, the chk2 inhibitor hardly affected the radiation-induced G2 population in A549 cells (Figure 6B).

6. Involvement of checkpoint kinases in the regulation of radioresistance

Since we found that chk1 is essential for the radiation-induced G2 arrest (Figure 6A), we investigated whether chk1 is involved in the radioresistance of human LUAD cell lines. As shown in Figure 7, the chk1 inhibitor was able to decrease the surviving fraction of the irradiated H1299 cells (when compared with the DMSO treatment), whereas there was no significant difference between the DMSO- and the chk1 inhibitor-treated irradiated A549 cells. Although the chk2 inhibitor alone also failed to decrease the surviving fraction of the irradiated A549 cells, a cotreatment with the chk1 and the chk2 inhibitors significantly decreased the surviving fraction of the irradiated A549 cells (Figure 7 left). These findings suggest that the chk1-mediated G2 arrest contributes to the radioresistance of H1299 cells, whereas the chk2-mediated events as well as the chk1-mediated G2 arrest are involved

in the radioresistance of the A549 cells.

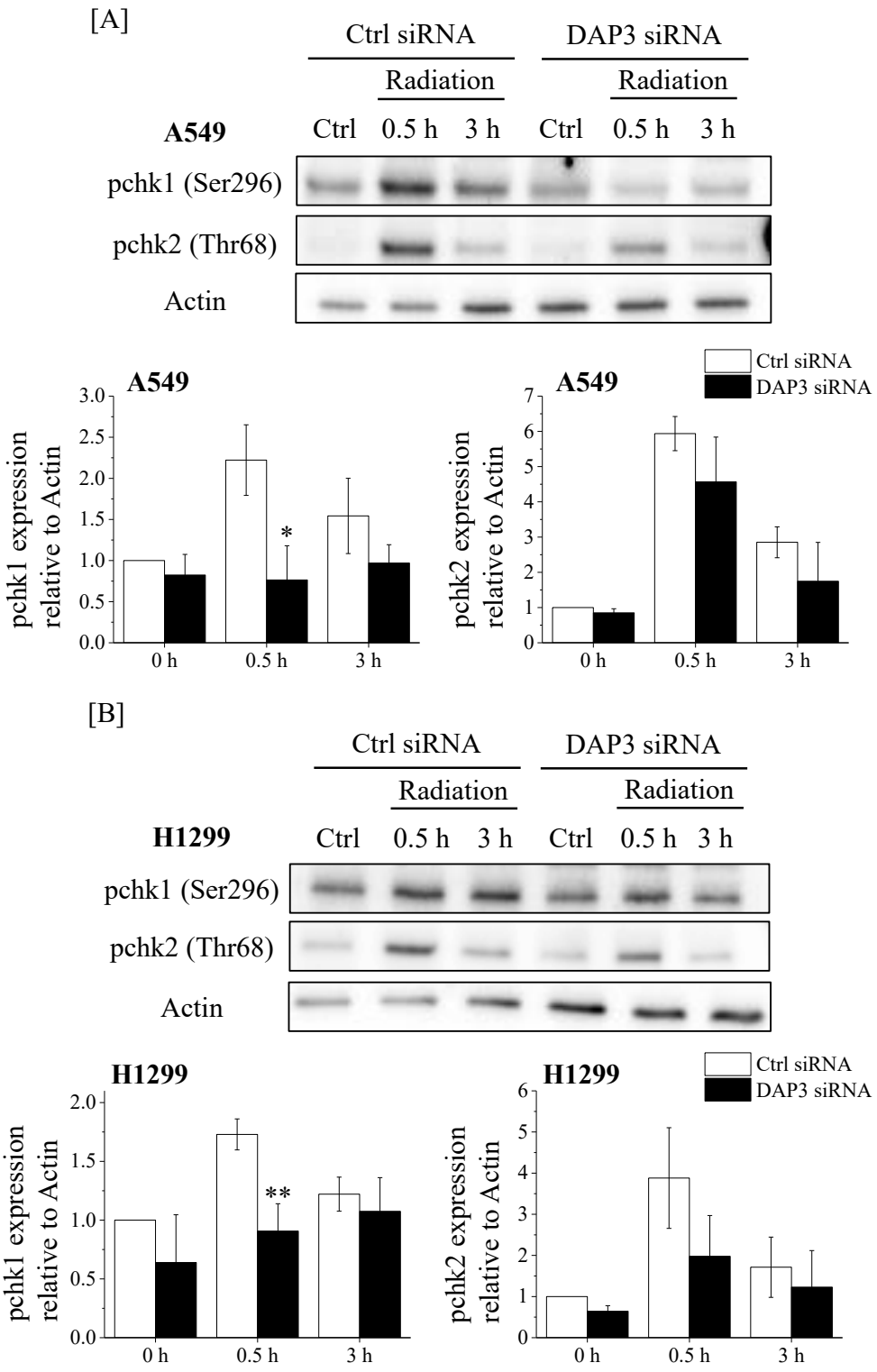

Figure 5. Effects of DAP3 knockdown on the expression of checkpoint kinases in irradiated human LUAD cell lines. (**A,B**) A549 (**A**) and H1299 (**B**) cells transfected with control or DAP3 siRNA were treated with 4-Gy irradiation, and were cultured for 0.5 or 3 h. The cells were harvested for the undertaking of Western blot analysis. A representative image of an immunoblot is shown.

Actin was used as the loading control. The relative values of the pchk1/actin and the pchk2/actin ratios are presented, where pchk1 and pchk2 indicate the phosphorylated-chk1 and the phosphorylated-chk2, respectively. Symbols used: *, $p < 0.05$, and **, $p < 0.01$; both versus control siRNA.

[A]

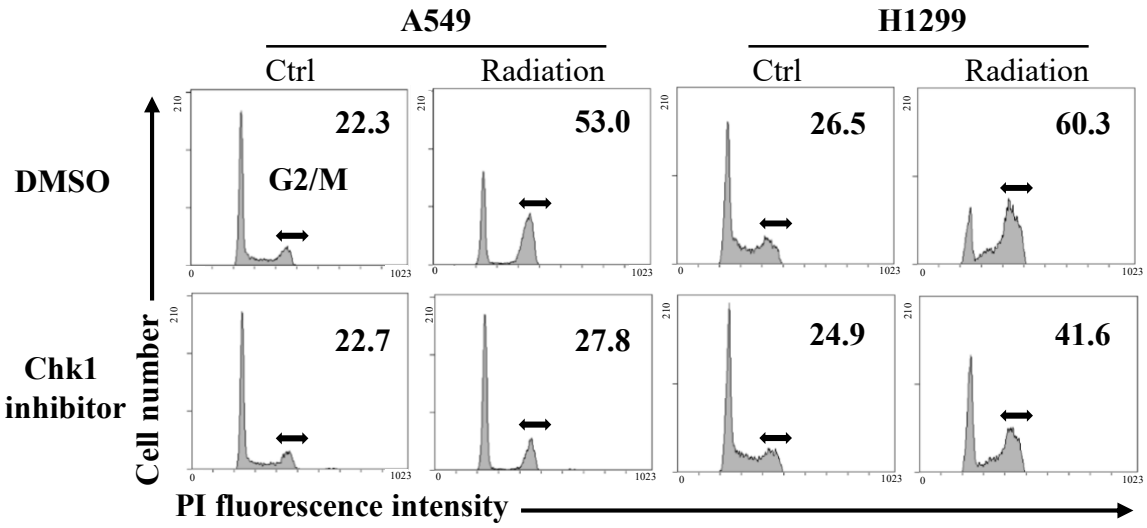

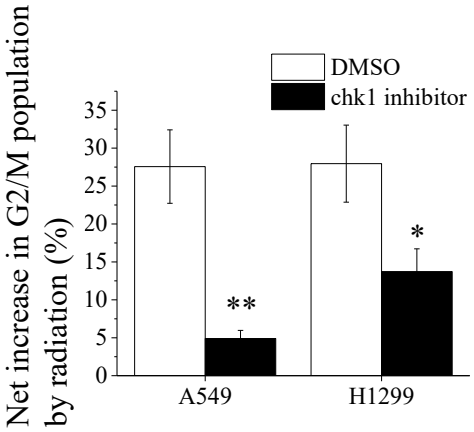

[B]

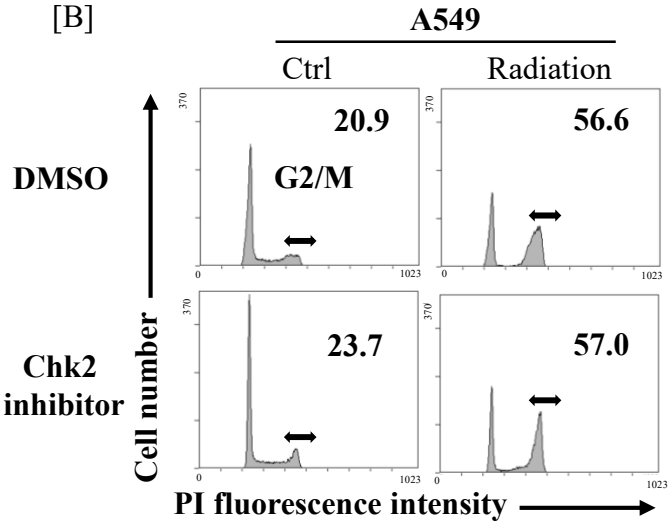

Figure 6. Involvement of chk1 in radiation-induced G2/M arrest in human LUAD cell lines. (**A**) Human LUAD cell lines were incubated with DMSO or with a chk1 inhibitor. After incubation for 1 h, the cells were irradiated (4 Gy). After 8 h of culturing, the cells were harvested for the undertaking of cell cycle analysis. (**Top**) Representative histograms and the obtained data are presented. Double-headed arrows indicate the G2/M population, while the inset number in the figure indicates the G2/M proportion in the total cells. (**Bottom**) The net increase in G2/M populations as a result of the undertaken irradiation is shown. Symbols used: *, $p < 0.05$, and **, $p < 0.01$; both versus DMSO. (**B**) A549 cells treated with DMSO or with a chk2 inhibitor were cultured for 8 h. The cells were harvested for the undertaking of cell cycle analysis. Representative histograms and the obtained data are presented. Double-headed arrows indicate the G2/M population, while the inset number in the figure indicates the G2/M proportion in the total cells.

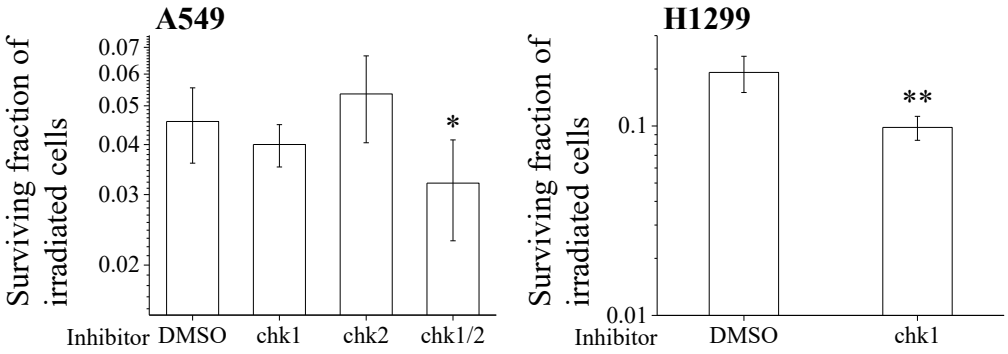

Figure 7. Involvement of checkpoint kinases in the radioresistance of human LUAD cell lines. (**Left**) A549 cells were incubated with DMSO or with a chk1 and/or a chk2 inhibitor and (**Right**) H1299 cells were incubated with DMSO or with a chk1 inhibitor. After an incubation for 1 h, the cells were irradiated (6 Gy). After 24 h of culturing, the cells were harvested and seeded for the undertaking of colony formation assays. The results are shown as the surviving fraction of human LUAD cell lines. Symbols used: *, $p < 0.05$, and **, $p < 0.01$; both versus DMSO.

7. Reduction of the radiation-induced p21 expression by the DAP3 knockdown

We finally explored the chk2-mediated events that can potentially contribute to the radioresistance of A549 cells. We have, herein, focused on p21, which is known to regulate radioresistance and be induced by a chk2-mediated pathway[59,68,69]. As shown in Figure 8, the expression of p21 was increased at 24 h after irradiation. Notably, a cotreatment with the chk1 and the chk2 inhibitors resulted in a decrease of the radiation-induced p21 expression.

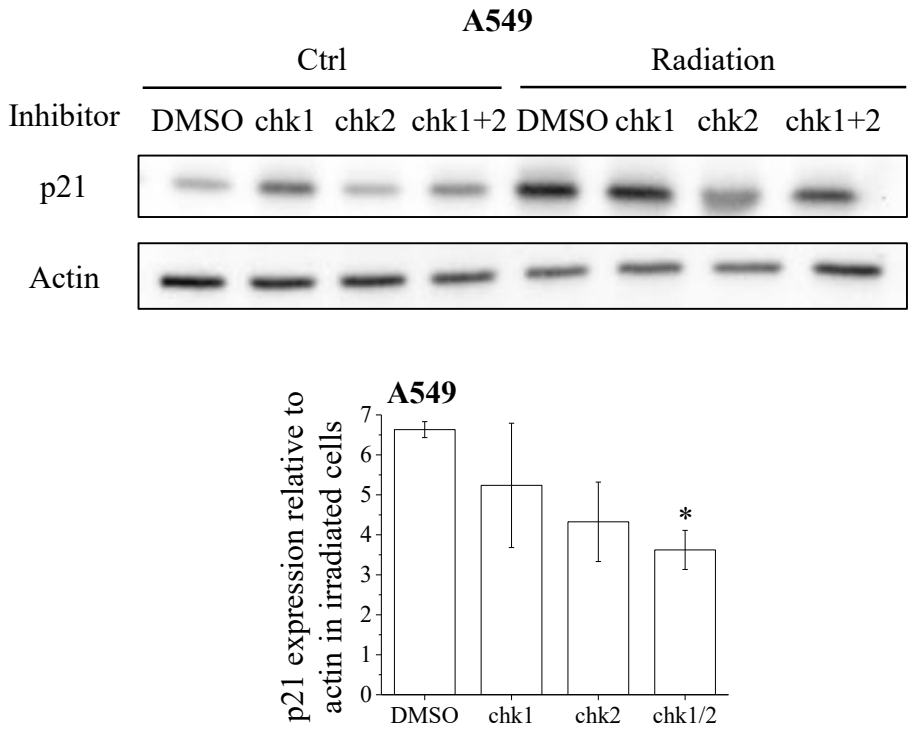

Figure 8. Effects of checkpoint kinase inhibitors on the radiation-induced p21 expression in A549 cells. A549 cells were incubated with DMSO or with a chk1 and/or a chk2 inhibitor. After an incubation for 1 h, the cells were irradiated (8 Gy). The cells were harvested for the undertaking of Western blot analysis. A representative image of an immunoblot is shown. Actin was used as the loading control. Symbols used: *, $p < 0.05$ versus DMSO.

Discussion

DAP3 is known as a mediator of apoptosis induced by interferon-gamma, the Fas ligand, and the tumor necrosis factor alpha[18,40]. However, recent studies have revealed a pro-survival and oncogenic function of DAP3[70,71]. For example, Wazir et al. have recently reported that a DAP3 knockdown can inhibit the growth of breast cancer cells[70]. In addition, Han et al. have shown that the subcutaneous injection of a DAP3-depleted esophageal squamous cell carcinoma cell line into mice can lead to the formation of much smaller tumors (when compared to those formed by the injection of control cells) [71]. An analysis using a public database has revealed that the expression levels of the *DAP3* mRNA in LUAD tissue are significantly higher than those in normal tissue (Supplementary Figure 1A), and that LUAD patients with high mRNA expressions of *DAP3* have poor outcomes (Supplementary Figure 1B). In addition, DAP3 knockdown A549 and H1299 cells display a lower ability of colony formation compared to control cells (Supplementary Figure 1C). Taken together, these findings suggest that DAP3 could serve as a potential therapeutic target for LUAD as well as for other tumors.

Although our previous report has shown that DAP3 could be an effective target for the improvement of the radiosensitivity of human LUAD cells[56], the molecular mechanisms underlying the DAP3-mediated radioresistance of LUAD cells remains unclear. Hence, we have herein investigated the involvement of DAP3 in the radiation-induced cell cycle arrest, as well as its role in the radioresistance of human LUAD cell lines. Our findings demonstrate that the DAP3 knockdown decreases the radiation-induced G2 arrest and the expression of proteins related to the cell cycle arrest such as pcdc2 and pchk1. Additionally, our experiments with the use of chk1 and chk2 inhibitors have shown that chk1 regulates the radioresistance of H1299 cells through a G2 arrest, whereas both the chk1-mediated G2 arrest and the chk2-mediated events may contribute to the radioresistance of A549 cells.

DAP3 is known to be involved in the mitochondrial ribosomal function, cell death, and RNA editing [18,40,43,71]. As far as we know, this is the first study demonstrating that DAP3 is involved in the radiation-induced G2 arrest through the phosphorylation of chk1, despite the fact that it remains unclear how DAP3 regulates the radiation-induced pchk1. Since ataxia-telangiectasia mutated (ATM) as well as ATM and RAD3-related (ATR) participate in the regulation of chk1 and chk2 phosphorylation[72], it is possible that DAP3 might control the radiation-induced pchk1 through the regulation of ATM or of ATR. In addition, there is another possibility that the mitochondrial ribosomal function of DAP3 (i.e., the ATP production) is involved in the regulation of radiation-induced pchk1, as the ATP is essential for phosphorylation and the DAP3 knockdown is known to decrease the ATP production[43]. Therefore, further studies are required in order to explore these possibilities.

Cell cycle checkpoints are promising targets for the sensitization of cancer cells to radiation,

and many studies have shown that by abrogating a G2 arrest one can sensitize a panel of human cancer cells to radiation[73-75]. For example, Patel et al. have shown that the radiosensitizing effect of the chk1 inhibitor CCT244747 was elicited by the abrogation of the radiation-induced G2 arrest[74]. In addition, Liu et al. have revealed a negative correlation of the cellular radiosensitivity with the accumulated the G2/M arrested cells[76]. Therefore, it is likely that the DAP3 knockdown-induced abrogation of G2 arrest might at least be partially involved in the enhancement of radiosensitivity induced by the DAP3 knockdown.

We have, herein, also identified a differential effect of the chk1 inhibitor on the radiosensitivity of A549 and of H1299 cells. Bridge et al. have reported that MK-8776 (another name for the chk1 inhibitor used in this study) was able to radiosensitize p53-defective cancer cell lines, but not cell lines with wild-type p53, deriving from human non-small cell lung cancer and human head and neck squamous cell carcinomas[75]. Furthermore, Borst et al. have reported that the chk1 inhibitor SAR020106 can enhance radiosensitivity in p53-deficient Cal27, HN6, and HeLa cells, but not in p53 wild-type A549 cells[77]. p53 is a transcription factor that regulates many biological pathways, including those involved in DNA repair as well as the chk1-mediated pathway leading to cell cycle arrest[58,78]. Since A549 cells contain wild-type p53[77], whereas H1299 cells contain no p53 gene[75], the different effect of the chk1 inhibitor on the radiosensitivity of A549 and of H1299 cells may be attributed to the difference in terms of their p53 status.

It is well known that chk2 regulates p53-related pathways such as that also mediated by p21, which has been reported to be involved in the radioresistance of various tumor types, including some of those occurring in the lungs, the brain, the prostate, the cervix, the esophagus, and the large intestine, as well as in nasopharyngeal carcinoma. For example, p53-p21 is known to mediate cell cycle G1 arrest, senescence, and glycolysis under hypoxia[69]. Since a cotreatment with a chk1 and a chk2 inhibitor can enhance the radiosensitivity of A549 cells along with the induction of a decrease in radiation-induced p21 expression, it is possible that p21 might be involved in DAP3-mediated radioresistance. Of course, one cannot exclude the possibility that factors other than p21 might contribute to the DAP3-mediated radioresistance, as the p53-chk2 pathway regulates many signaling pathways[69].

In conclusion, our findings reveal a novel role of DAP3 to regulate G2 arrest through pchk1 in irradiated LUAD cells. In addition, the present results suggested that a G2 arrest can regulate the radioresistance of H1299 cells, whereas both the chk1-mediated G2 arrest and the chk2-mediated events may contribute to the radioresistance of A549 cells. We hope that these findings related to radioresistance might improve the efficacy of radiotherapy for human LUAD.

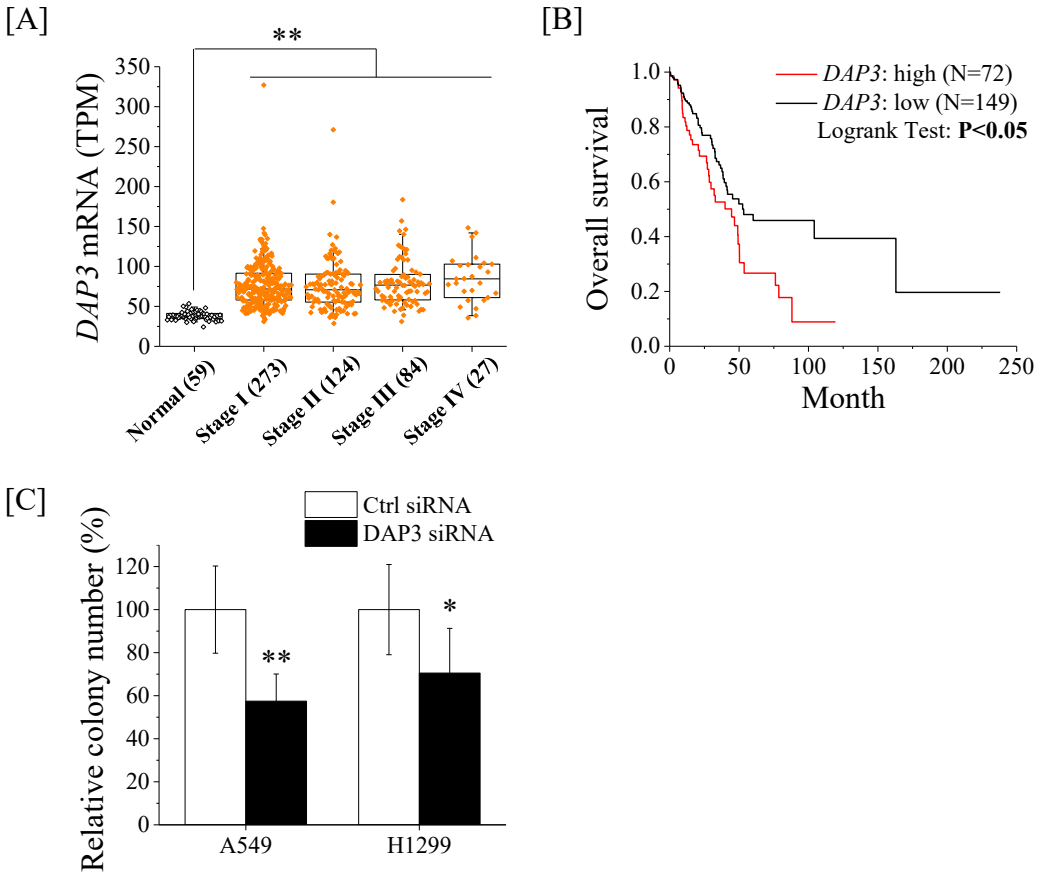

Supplementary Figure 1. Association between DAP3 and human LUAD malignancies. (**A**) Expression levels of *DAP3* mRNA in human LUAD tissues and adjacent normal tissues are shown. (**B**) The relationship between the overall survival and the DAP3 expression of human LUAD patients in TCGA cohorts is shown. (**C**) The clonogenic potential of human LUAD cells transfected with control or DAP3 siRNA was assessed by a colony formation assay. The number of colonies formed by non-irradiated cells transfected with control siRNA was considered as 100%. Data are presented as the mean ± SD of at least three independent experiments. Symbols used: *, $p < 0.05$, and **, $p < 0.01$; both versus control siRNA.

謝辞

本研究の遂行に際し，終始ご懇篤なるご指導とご鞭撻を賜りました弘前大学大学院保健学研究科放射線技術科学領域 柏倉幾郎　教授，敦賀英知　教授，吉野浩教　助教に深く感謝申し上げます.

References

1) Suen D.F., Norris K.L., Youle R.J. Mitochondrial dynamics and apoptosis. Genes Dev., 22:1577-1590, 2008.
2) Angajala A., Lim S., Phillips J.B., Kim J.H., Yates C., You Z., Tan M. Diverse roles of mitochondria in immune responses: Novel insights into immuno-metabolism. *Front. Immunol.,* 9:1605, 2018.
3) Senft D., Ronai Z.A. Regulators of mitochondrial dynamics in cancer. *Curr. Opin. Cell Biol.,* 39:43–52, 2016.
4) Mishra P., Chan D.C. Mitochondrial dynamics and inheritance during cell division, development and disease. *Nat. Rev. Mol. Cell Biol.,* 15:634–646, 2014.
5) Castanier C., Garcin D., Vazquez A., Arnoult D. Mitochondrial dynamics regulate the RIG-I-like receptor antiviral pathway. *EMBO Rep.,* 11:133–138, 2010.
6) Kobashigawa S., Suzuki K., Yamashita S. Ionizing radiation accelerates Drp1-dependent mitochondrial fission, which involves delayed mitochondrial reactive oxygen species production in normal human fibroblast-like cells. *Biochem. Biophys. Res. Commun.,* 414:795–800, 2011.
7) Kwon S.M., Lee Y.K., Min S., Woo H.G., Wang H.J., Yoon G. Mitoribosome defect in hepatocellular carcinoma promotes an aggressive phenotype with suppressed immune reaction. *iScience.,* 23:101247, 2020.
8) Yoneyama M., Fujita T. Structural mechanism of RNA recognition by the RIG-I-like receptors. *Immunity.,* 29:178–181, 2008
9) Kawai T., Takahashi K., Sato S., Coban C., Kumar H., Kato H., Ishii K.J., Takeuchi O., Akira S. IPS-1, an adaptor triggering RIG-I- and Mda5-mediated type I interferon induction. *Nat. Immunol.,* 6:981–988, 2005.
10) Besch R., Poeck H., Hohenauer T., Senft D., Häcker G., Berking C., Hornung V., Endres S., Ruzicka T., Rothenfusser S., et al. Proapoptotic signaling induced by RIG-I and MDA-5 results in type I interferon-independent apoptosis in human melanoma cells. *J. Clin. Investig.,* 119:2399–2411, 2009.
11) Wu Y., Wu X., Wu L., Wang X., Liu Z. The anticancer functions of RIG-I–like receptors, RIG-I and MDA5, and their applications in cancer therapy. *Transl. Res.,* 190:51–60, 2017.
12) Yuan D., Xia M., Meng G., Xu C., Song Y., Wei J. Anti-angiogenic efficacy of 5'-triphosphate siRNA combining VEGF silencing and RIG-I activation in NSCLCs. *Oncotarget.,* 6:29664–29674, 2015.
13) Poeck H., Besch R., Maihoefer C., Renn M., Tormo D., Morskaya S.S., Kirschnek S., Gaffal E., Landsberg J., Hellmuth J., et al. 5'-triphosphate-siRNA: Turning gene silencing and Rig-I

activation against melanoma. *Nat. Med.,* 14:1256–1263, 2008.

14) Li D., Gale R.P., Liu Y., Lei B., Wang Y., Diao D., Zhang M. 5′-Triphosphate siRNA targeting MDR1 reverses multi-drug resistance and activates RIG-I-induced immune-stimulatory and apoptotic effects against human myeloid leukaemia cells. *Leuk. Res.,* 58:23–30, 2017.
15) Yoshino H., Iwabuchi M., Kazama Y., Furukawa M., Kashiwakura I. Effects of retinoic acid-inducible gene-I-like receptors activations and ionizing radiation cotreatment on cytotoxicity against human non-small cell lung cancer in vitro. *Oncol. Lett.,* 15:4697–4705, 2018.
16) Bo T., Yamamori T., Yamamoto K., Fujimoto M., Yasui H., Inanami O. Mitochondrial fission promotes radiation-induced increase in intracellular Ca^{2+} level leading to mitotic catastrophe in mouse breast cancer EMT6 cells. *Biochem. Biophys. Res. Commun.,* 522:144–150, 2020.
17) Kim S.J., Syed G.H., Khan M., Chiu W.W., Sohail M.A., Gish R.G., Siddiqui A. Hepatitis C virus triggers mitochondrial fission and attenuates apoptosis to promote viral persistence. *Proc. Natl. Acad. Sci.,* 111:6413–6418, 2014.
18) Kissil J.L., Cohen O., Raveh T., Kimchi A. Structure-function analysis of an evolutionary conserved protein, DAP3, which mediates TNF-alpha- and Fas-induced cell death. *EMBO J.,* 18:353–362, 1999.
19) Henning K.A. *Ph.D. Thesis.* Stanford University; Palo Alto, CA, USA: 1992. The Molecular Genetics of Human Diseases with Defective DNA Damaging Processing.
20) Yoshino H., Kumai Y., Kashiwakura I. Effects of endoplasmic reticulum stress on apoptosis induction in radioresistant macrophages. *Mol. Med. Rep.,* 15:2867–2872, 2017.
21) Sato Y., Yoshino H., Kazama Y., Kashiwakura I. Involvement of caspase-8 in apoptosis enhancement by cotreatment with retinoic acid-inducible gene-I-like receptor agonist and ionizing radiation in human non-small cell lung cancer. *Mol. Med. Rep.,* 18:5286–5294, 2018.
22) Yoshino H., Kashiwakura I. Involvement of reactive oxygen species in ionizing radiation–induced upregulation of cell surface Toll-like receptor 2 and 4 expression in human monocytic cells. *J. Radiat. Res.,* 58:626–635, 2017.
23) Yoshino H., Konno H., Ogura K., Sato Y., Kashiwakura I. Relationship between the regulation of caspase-8-mediated apoptosis and radioresistance in human THP-1-derived macrophages. *Int. J. Mol. Sci.,* 19:3154, 2018.
24) Ishihara N., Fujita Y., Oka T., Mihara K. Regulation of Mitochondrial Morphology through Proteolytic Cleavage of OPA1. *EMBO J.,* 25:2966–2977, 2006.
25) García M.A., Meurs E.F., Esteban M. The dsRNA protein kinase PKR: Virus and cell control. *Biochimie.,* 89:799–811, 2007.
26) Elion D.L., Cook R.S. Harnessing RIG-I and intrinsic immunity in the tumor microenvironment for therapeutic cancer treatment. *Oncotarget.,* 9:29007–29017, 2018.

27) Monlun M., Hyernard C., Blanco P., Lartigue L., Faustin B. Mitochondria as molecular platforms integrating multiple innate immune signalings. *J. Mol. Biol.,* 429:1–13, 2017.
28) Kim S.J., Ahn D.G., Syed G.H., Siddiqui A. The essential role of mitochondrial dynamics in antiviral immunity. *Mitochondrion.,* 41:21–27, 2018.
29) Barbier V., Lang D., Valois S., Rothman A.L., Medin C.L. Dengue virus induces mitochondrial elongation through impairment of Drp1-triggered mitochondrial fission. *Virology.,* 500:149–160, 2017.
30) Fields J.A., Serger E., Campos S., Divakaruni A.S., Kim C., Smith K., Trejo M., Adame A., Spencer B., Rockenstein E., et al. HIV alters neuronal mitochondrial fission/fusion in the brain during HIV-associated neurocognitive disorders. *Neurobiol. Dis.,* 86:154–169, 2016.
31) Berg R.K., Melchjorsen J., Rintahaka J., Diget E., Søby S., Horan K.A., Gorelick R.J., Matikainen S., Larsen C.S., Ostergaard L., et al. Genomic HIV RNA Induces Innate Immune Responses through RIG-I-Dependent Sensing of Secondary-Structured RNA. *PLoS ONE.,* 7:e29291, 2012.
32) Sprokholt J.K., Kaptein T.M., van Hamme J.L., Overmars R.J., Gringhuis S.I., Geijtenbeek T.B.H. RIG-I-like receptor activation by dengue virus drives follicular T helper cell formation and antibody production. *PLoS Pathog.,* 13:e1006738. 2017.
33) Saita S., Ishihara T., Maeda M., Iemura S., Natsume T., Mihara K., Ishihara N. Distinct types of protease systems are involved in homeostasis regulation of mitochondrial morphology via balanced fusion and fission. *Genes Cells.,* 21:408–424, 2016.
34) Kobashigawa S., Kashino G., Suzuki K., Yamashita S., Mori H. Ionizing radiation-induced cell death is partly caused by increase of mitochondrial reactive oxygen species in normal human fibroblast cells. *Radiat. Res.,* 183:455–464, 2015.
35) Xu W., Jing L., Wang Q., Lin C.C., Chen X., Diao J., Liu Y., Sun X. Bax-PGAM5L-Drp1 complex is required for intrinsic apoptosis execution. *Oncotarget,* 6:30017–30034, 2015.
36) Rong R., Xia X., Peng H., Li H., You M., Liang Z., Yao F., Yao X., Xiong K., Huang J., et al. Cdk5-mediated Drp1 phosphorylation drives mitochondrial defects and neuronal apoptosis in radiation-induced optic neuropathy. *Cell Death Dis.,* 11:1–17, 2020.
37) Inoue-Yamauchi A., Oda H. Depletion of mitochondrial fission factor DRP1 causes increased apoptosis in human colon cancer cells. *Biochem. Biophys. Res. Commun.,* 421:81–85, 2012.
38) Cheng W.Y., Chow K.C., Chiao M.T., Yang Y.C., Shen C.C. Reducing expression of dynamin-related protein 1 increases radiation sensitivity of glioblastoma cells. *BioRxiv.,* 688861, 2019.
39) Akita M., Suzuki-Karasaki M., Fujiwara K., Nakagawa C., Soma M., Yoshida Y., Ochiai T., Tokuhashi Y., Suzuki-Karasaki Y. Mitochondrial division inhibitor-1 induces mitochondrial hyperfusion and sensitizes human cancer cells to TRAIL-induced apoptosis. *Int. J.*

Oncol., 45:1901–1912, 2014.

40) Kissil J.L., Deiss L.P., Bayewitch M., Raveh T., Khaspekov G., Kimchi A. Isolation of DAP3, a novel mediator of interferon-gamma-induced cell death. *J. Biol. Chem.* 1995;270:27932–27936.
41) Miyazaki T., Shen M., Fujikura D., Tosa N., Kim H.R., Kon S., Uede T., Reed J.C. Functional role of death-associated protein 3 (DAP3) in anoikis. *J. Biol. Chem.,* 279:44667–44672, 2004.
42) Miyazaki T., Reed J.C. A GTP-binding adapter protein couples TRAIL receptors to apoptosis-inducing proteins. *Nat. Immunol.,* 2:493–500, 2001.
43) Xiao L., Xian H., Lee K.Y., Xiao B., Wang H., Yu F., Shen H.M., Liou Y.C. Death-associated protein 3 regulates mitochondrial-encoded protein synthesis and mitochondrial dynamics. *J. Biol. Chem.,* 290:24961–24974, 2015.
44) Wang J.X., Li Q., Li P.F. Apoptosis Repressor with Caspase Recruitment Domain Contributes to Chemotherapy Resistance by Abolishing Mitochondrial Fission Mediated by Dynamin-Related Protein-1. *Cancer Res.,* 69:492–500, 2009.
45) Landes T., Martinou J.C. Mitochondrial outer membrane permeabilization during apoptosis: The role of mitochondrial fission. *Biochim. Biophys. Acta.,* 1813:540–545, 2011.
46) Tang L., Wei F., Wu Y., He Y., Shi L., Xiong F., Gong Z., Guo C., Li X., Deng H., et al. Role of metabolism in cancer cell radioresistance and radiosensitization methods. *J. Exp. Clin. Cancer Res.,* 37:87, 2018.
47) Wang Y., Hou Q., Xiao G., Yang S., Di C., Si J., Zhou R., Ye Y., Zhang Y., Zhang H. Selective ATP hydrolysis inhibition in F1Fo ATP synthase enhances radiosensitivity in non-small-cell lung cancer cells (A549) *Oncotarget,* 8:53602–53612, 2017.
48) Jacques C., Chevrollier A., Loiseau D., Lagoutte L., Savagner F., Malthièry Y., Reynier P. mtDNA controls expression of the death associated protein 3. *Exp. Cell Res.* 2006;312:737–745.
49) Casula M., Bosboom-Dobbelaer I., Smolders K., Otto S., Bakker M., de Baar M.P., Reiss P., de Ronde A. Infection with HIV-1 induces a decrease in mtDNA. *J. Infect. Dis.,* 191:1468–1471, 2005.
50) Siegel RL, Miller KD, Fuchs HE et al. Cancer Statistics, 2021. *CA Cancer J Clin,* 71:7–33, 2021.
51) Butnor KJ. Controversies and challenges in the histologic subtyping of lung adenocarcinoma. *Transl Lung Cancer Res,* 9:839–46, 2020.
52) Luo Y-H, Luo L, Wampfler JA et al. 5-year overall survival in patients with lung cancer eligible or ineligible for screening according to US Preventive Services Task Force criteria: a prospective, observational cohort study. *Lancet Oncol*, 20:1098–108, 2019.
53) Huang G, Li H, Zhang H. Abnormal expression of mitochondrial ribosomal proteins and their encoding genes with cell apoptosis and diseases. *Int J Mol Sci*, 21:8879, 2020.
54) Malladi S, Parsa KVL, Bhupathi D et al. Deletion mutational analysis of BMRP, a pro-apoptotic

protein that binds to Bcl-2. *Mol Cell Biochem* 2011;351:217–32.

55) Wang Z, Li J, Long X *et al.* MRPS16 facilitates tumor progression via the PI3K/AKT/Snail signaling axis. *J Cancer* 2020;**11**:2032–43.

56) Sato Y, Yoshino H, Kashiwakura I et al. DAP3 Is Involved in modulation of cellular radiation response by RIG-I-like receptor agonist in human lung adenocarcinoma cells. *Int J Mol Sci*, 22:420, 2021.

57) Mao Z, Bozzella M, Seluanov A et al. DNA repair by nonhomologous end joining and homologous recombination during cell cycle in human cells. *Cell Cycle*, 7:2902–6, 2008.

58) Smith HL, Southgate H, Tweddle DA *et al.* DNA damage checkpoint kinases in cancer. *Expert Rev Mol Med*, 22:e2, 2020.

59) Otto T, Sicinski P. Cell cycle proteins as promising targets in cancer therapy. *Nat Rev Cancer*, 17:93–115, 2017.

60) Wang J, Gu Q, Li M et al. Identification of XAF1 as a novel cell cycle regulator through modulating G(2)/M checkpoint and interaction with checkpoint kinase 1 in gastrointestinal cancer. *Carcinogenesis*, 30:1507–16, 2009.

61) Huang Y, Tian Y, Zhang W et al. Rab12 promotes radioresistance of HPV-positive cervical cancer cells by increasing G2/M arrest. *Front Oncol*, 11:586771, 2021.

62) Guzi TJ, Paruch K, Dwyer MP et al. Targeting the replication checkpoint using SCH 900776, a potent and functionally selective CHK1 inhibitor identified via high content screening. *Mol Cancer Ther*, 10:591–602, 2011.

63) Arienti KL, Brunmark A, Axe FU et al. Checkpoint kinase inhibitors: SAR and radioprotective properties of a series of 2-arylbenzimidazoles. *J Med Chem*, 48:1873–85, 2005.

64) Wakasaya T, Yoshino H, Fukushi Y et al. A liquid crystal-related compound induces cell cycle arrest at the G2/M phase and apoptosis in the A549 human non-small cell lung cancer cell line. *Int J Oncol*, 42:1205–11, 2013.

65) Castedo M, Perfettini J-L, Roumier T et al. Cell death by mitotic catastrophe: a molecular definition. *Oncogene*, 23:2825–37, 2004.

66) Vakifahmetoglu H, Olsson M, Zhivotovsky B. Death through a tragedy: mitotic catastrophe. *Cell Death Differ*, 15:1153–62, 2008.

67) Lauber K, Ernst A, Orth M et al. Dying cell clearance and its impact on the outcome of tumor radiotherapy. *Front Oncol*, 2:116, 2012.

68) Huang R-X, Zhou P-K. DNA damage response signaling pathways and targets for radiotherapy sensitization in cancer. *Signal Transduct Target Ther*, 5:60, 2020.

69) Kuang Y, Kang J, Li H et al. Multiple functions of p21 in cancer radiotherapy. J Cancer Res Clin Oncol, 147:987–1006, 2021.

70) Wazir U, Sanders AJ, Wazir AMA et al. Effects of the knockdown of death-associated protein 3 expression on cell adhesion, growth and migration in breast cancer cells. *Oncol Rep*, 33:2575–82, 2015.
71) Han J, An O, Hong H et al. Suppression of adenosine-to-inosine (A-to-I) RNA editome by death associated protein 3 (DAP3) promotes cancer progression. *Sci Adv*, 6:eaba5136, 2020.
72) Mladenov E, Fan X, Dueva R et al. Radiation-dose-dependent functional synergisms between ATM, ATR and DNA-PKcs in checkpoint control and resection in G2-phase. *Sci Rep*, 9:8255, 2019.
73) Suzuki M, Yamamori T, Bo T et al. MK-8776, a novel Chk1 inhibitor, exhibits an improved radiosensitizing effect compared to UCN-01 by exacerbating radiation-induced aberrant mitosis. *Transl Oncol*, 10:491–500, 2017.
74) Patel R, Barker HE, Kyula J et al. An orally bioavailable Chk1 inhibitor, CCT244747, sensitizes bladder and head and neck cancer cell lines to radiation. *Radiother Oncol*, 122:470–5, 2017.
75) Bridges KA, Chen X, Liu H et al. MK-8776, a novel chk1 kinase inhibitor, radiosensitizes p53-defective human tumor cells. *Oncotarget*, 7:71660–72, 2016.
76) Liu C, Nie J, Wang R et al. The cell cycle G2/M block is an indicator of cellular radiosensitivity. *Dose Response*, 17:1559325819891008, 2019.
77) Borst GR, McLaughlin M, Kyula JN et al. Targeted radiosensitization by the Chk1 inhibitor SAR-020106. *Int J Radiat Oncol Biol Phys*, 85:1110–8, 2013.
78) Wang XQ, Stanbridge EJ, Lao X et al. p53-dependent Chk1 phosphorylation is required for maintenance of prolonged G2 arrest. *Radiat Res*, 168:706–15, 2007.

要旨

ヒト肺腺癌細胞の放射線応答制御におけるミトコンドリア関連因子の役割に関する研究

佐藤　嘉晃
弘前大学大学院保健学研究科放射線技術科学領域

ミトコンドリアは融合と分裂を繰り返す動的な細胞小器官であり，独自の DNA やリボソームを有する．これらの特徴はウイルス感染や放射線などのストレスに対して自身の機能を維持するために重要な役割を果たしている．所属研究室ではこれまでに，ウイルス由来の核酸を認識して抗ウイルス応答を誘導する Retinoic acid-inducible gene-I (RIG-I) 様受容体 (RIG-I-like receptors: RLR) の刺激因子がヒト肺腺癌細胞の放射線応答を制御することを報告しているが，RLR 刺激因子による放射線応答制御機構とミトコンドリアとの関連は未解明である．

本研究でははじめに，ミトコンドリア融合・分裂因子と DAP3 のタンパク質発現を解析したところ，RLR 刺激因子を処理したヒト肺腺癌細胞 A549 ではこれらタンパク質の発現が減少していることを見出した．そこで，RNA 干渉法により調製した各タンパク質発現抑制細胞を用いて実験を行ったところ，(i) DAP3 がヒト肺腺癌細胞の放射線抵抗性に関与していること，(ii) DAP3 の発現抑制細胞では放射線による細胞死が増加し，その結果 Poly(I:C)による放射線誘発細胞死増強効果が減弱することが明らかとなった．

また，DAP3 を介した放射線抵抗性制御機構は未解明であったため，放射線抵抗性に関わる細胞周期および DNA 損傷応答制御と DAP3 との関連を解析したところ，(i) DAP3 の発現抑制により照射後のリン酸化 checkpoint kinase 1 (chk1) を介した G2/M 期停止が抑制されること，(ii) chk1 を介した G2/M 期停止が H1299 の放射線抵抗性を制御している一方で，chk1 を介した G2/M 期停止と chk2 を介したイベントが A549 の放射線抵抗性を制御していることが示唆された．

以上の結果より，RLR 刺激因子 Poly(I:C)は DAP3 のタンパク質発現を減少させることでヒト肺腺癌細胞の放射線応答を制御していることが示唆された．また，DAP3 は chk1 を介して放射線誘発 G2/M 期停止を誘導することで H1299 の放射線抵抗性を制御していることが示唆された．一方 A549 に対しては DAP3 が chk1 と chk2 を介したイベントを通して放射線抵抗性を制御している可能性が示唆された．